Summer 2005

Evaluation of coding scheme for MIMO radar

Suresh Kumar Harikrishnan
New Jersey Institute of Technology

Copyright Warning & Restrictions

The copyright law of the United States (Title 17, United States Code) governs the making of photocopies or other reproductions of copyrighted material.

Under certain conditions specified in the law, libraries and archives are authorized to furnish a photocopy or other reproduction. One of these specified conditions is that the photocopy or reproduction is not to be "used for any purpose other than private study, scholarship, or research." If a, user makes a request for, or later uses, a photocopy or reproduction for purposes in excess of "fair use" that user may be liable for copyright infringement,

This institution reserves the right to refuse to accept a copying order if, in its judgment, fulfillment of the order would involve violation of copyright law.

Please Note: The author retains the copyright while the New Jersey Institute of Technology reserves the right to distribute this thesis or dissertation

Printing note: If you do not wish to print this page, then select "Pages from: first page # to: last page #" on the print dialog screen

ABSTRACT

EVALUATION OF CODING SCHEME FOR MIMO RADAR

by
Suresh Kumar Harikrishnan

Multiple Input Multiple Output (MIMO) antenna systems have shown a great potential for wireless communication. These systems support high capacity, increased diversity and interference suppression. Recently it has been proposed MIMO constellations for Radar. MIMO Radar is not only a new research field, but also a very promising approach in terms of overcoming Radar Cross Section (RCS) fluctuations with diversity. This thesis explores the potential of coding schemes for MIMO Radar.

The ambiguity functions measures related to MIMO Radar are used to evaluate how much diversity gain can be coherently achieved with certain coding schemes. The results of this analysis show that the cross correlation between the signals from different transmitters hinders achieving the full diversity gain. The code length of the used Gold codes is an important factor for this effect.

However, in this thesis a coding scheme related to the Alamouti scheme in Communication is presented, this scheme under some constraints is capable of maintaining orthogonality between the signals from different transmitters and therefore cancels the mutual interference among those signals.

In general, MIMO radar is a novel and ingenious approach to improve radar performance which needs to be analyzed and developed. This thesis is the first work exploring the coding schemes and the related aspects for MIMO Radar.

EVALUATION OF CODING SCHEME FOR MIMO RADAR

by
Suresh Kumar Harikrishnan

A Thesis
Submitted to the Faculty of
New Jersey Institute of Technology
in Partial Fulfillment of the Requirements for the Degree of
Master of Science in Telecommunications

Department of Electrical and Computer Engineering

August 2005

APPROVAL PAGE

EVALUATION OF CODING SCHEME FOR MIMO RADAR

Suresh K. Harikrishnan

Dr. Alexander M. Haimovich, Thesis Advisor — Date
Professor of Electrical and Computer Engineering, NJIT

Dr. Ali N. Akansu, Committee Member — Date
Professor of Electrical and Computer Engineering, NJIT

Dr. Roy R. You, Committee Member — Date
Assistant Professor of Electrical and Computer Engineering, NJIT

BIOGRAPHICAL SKETCH

Author: Suresh Kumar Harikrishnan

Degree: Master of Science

Date: August 2005

Undergraduate and Graduate Education:

- Master of Science in Telecommunications,
  New Jersey Institute of Technology, Newark, NJ, 2005

- Bachelor of Technology in Electrical Engineering,
  Indian Institute of Technology, Madras, India, 2002

Major: Telecommunications

To my father for his guidance,
To my mother for her unconditional love,

ACKNOWLEDGEMENT

I would like to express my deepest appreciation to Dr. Alexander Haimovich, who not only served as my research supervisor, providing valuable and countless resources, insight, and intuition, but also constantly gave me support, encouragement, and reassurance. Special thanks are given to Dr. Ali N. Akansu and Dr. Roy R. You for actively participating in my committee.

I would like to take the opportunity to acknowledge the immense help and encouragement from Mr. Nikolaus Lehmann and many of my senior colleagues at the Center for Communication and Signal Processing Research Laboratory. Also, many thanks to Ms. Marlene Toeroek for her assistance in lab and the entire staff of Electrical and Computer Engineering Department at NJIT.

TABLE OF CONTENTS

TABLE OF CONTENTS
(Continued)

LIST OF TABLES

LIST OF FIGURES

LIST OF FIGURES
(Continued)

CHAPTER 1

INTRODUCTION

In this chapter a brief introduction to RADAR (Radio Detection and Ranging) is provided where a brief overview of Radar History, Technology and properties of Range resolution, Doppler resolution and Waveform design are discussed. Waveforms used in different radar application are also introduced. This chapter starts with the objective of the thesis and then proceeds with Radar fundamentals.

1.1 Objective of MIMO Radar Ambiguity Function

The objective of the thesis is to investigate and study the ambiguity function of MIMO (Multiple Input Multiple Output) Radar. Phase Coded Signals are transmitted from multiple transmitters and each illuminates different aspects of the target. At the receiver the signals are matched and filtered to get the target characteristics. The output of the matched filter is the ambiguity function, which is discussed in detail in chapter 2. The ambiguity function is then analyzed using multiple transmitters and by varying the code length of transmitted waveform. The advantages are weighed against conventional radar. Alamouti space-time codes are also examined for MIMO radar.

1.2 Radar History

In 19th century, researchers discovered that if an alternating electric current were run through a wire or rod, it emitted an invisible form of radiation that could generate an alternating electric current in a separate wire or rod. This invisible radiation was quickly realized to be a form of "electromagnetic radiation", a disturbance of electric and

magnetic fields that propagated through space. Since electromagnetic radiation is a wave phenomenon, it has certain characteristics associated with waves, such as polarization, phase, and wave interference. This radiation propagates at 300,000,000 meters per second.

Radar is a device that sends out electromagnetic waves. These waves reflect off objects in space, and a proportion of the original wave energy is actually bounced back towards the Radar. The Radar then reads this returning signal and analyzes it. The radar receiver extracts target information such as range, velocity, angular position and other target identifying characteristics and then processes these echoes.

Radar systems use modulated waveforms and directive antennas to transmit electromagnetic energy into a specific volume in space to search for targets. Objects (targets) within a search volume will reflect a part of this energy (radar returns or echoes) back to the radar.

Radar was initially theorized and investigated in the early 1920's by Dr. A. Hoyt Taylor at the Naval Research Laboratory in Washington D.C. Radar research was also carried out simultaneously in a variety of institutions in the U.S. and the U.K. The idea of using rays to kill or disable people or machines was very popular. Mr. Watson-Watt, Superintendent of the Radio Research Station at Slough, U.K was asked his views on the possibility of developing a radio "Death Ray" to melt metal or incapacitate an aircraft pilot. He reported that there was no possibility of achieving these destructive effects at a distance but that energy reflected from aircraft should be detectable at useful ranges. Thus a system of radiolocation using a pulse/echo technique was born. Robert Wilson-Watt created the first pulsed radio wave system in 1935. Radar developed rapidly during

the Second World War. During this time, it was noticed that the radar beam also echoed from precipitation. This proved to be a valuable tool in dictating military operations. After the war ended, de-classification allowed for a wider range of interested parties to experiment with radar technology. During the 1950s, the original weather service radar was deployed, primarily for the study of Tornadoes.

Radars can be classified based on their functionality, frequency band, antenna type, waveforms utilized and the location where they are used. They are utilized in a variety of applications viz weather tracking, search, tracking of targets, fire control, terrain following and terrain avoidance.

1.3 Types of Radar Waveforms

Radars are classified by the type of waveform they use. They can be classified as Continuous wave (CW) or Pulsed radars (PR). Perhaps the simplest radar waveform is the CW waveform. In this case, the transmitter typically broadcasts a continuous sinusoid while receiving target on a separate receiver antenna. The primary advantage of CW radar is unambiguous Doppler measurement, since each target velocity produces a single unique Doppler frequency shift of the CW carrier. Thus, unambiguous Doppler measurement permits reliable target separation based solely on Doppler frequency. However, in CW radar, the target range measurements are entirely ambiguous, i.e., the continuous nature of the radar waveform does not permit accurate estimation of unique range of information. If initial range is known, the radar may track range based on range-rate. However, initial range information is usually not available. Another disadvantage of CW radar, perhaps even greater than the ambiguous range problem, is the need for

separate transmitter/receiver antennas and problems associated with preventing transmitter leakage into the receiver [2].

Most modern radars employ a pulsed waveform. The primary advantage of pulsed radar over CW is that pulsing allows the transmitter and receiver to share the same antenna. Figure 1.1 illustrates the parameters associated with a typical pulsed radar waveform. The pulse duration, or pulse width (PW), is denoted as T_p and the pulse repetition interval (PRI) is denoted as T_r. From these fundamental waveform parameters, several other important parameters are derived. In general, pulsed radar transmits and receives a train of pulses. The Inter Pulse Period (IPP) is T and the pulse width is τ. The IPP is often referred to as Pulse Repetition Interval (PRI). The inverse of the PRI is the Pulse Repetition Factor (PRF), which is denoted by f_r,

$$f_r = \frac{1}{PRI} = \frac{1}{T} \tag{1.1}$$

During each PRI, the radar radiates energy only for τ seconds and listens for the target for the rest of the PRI. The radar transmitting duty cycle (factor) d_t is defined as the ratio

$$d_t = \frac{\tau}{T} \tag{1.2}$$

The radar average transmitting power is

$$P_{av} = P_t \text{ x } d_t \tag{1.3}$$

Where P_t denotes the radar peak transmitted power. The pulse energy is

$$E_p = P_t \text{ x } \tau = P_{av}T = \frac{P_{av}}{f_r} \tag{1.4}$$

The range corresponding to the two-way time delay T is known as the radar unambiguous range, R_u.

When wave 1 is transmitted as shown in Figure 1.1 and the received wave is of the form as shown in Figure 1.1 with a time delay Δt. The Echo pulse may be from a far away target due to pulse 1 or maybe from pulse 2 so there is a range ambiguity associated with the pulse being transmitted. This is called range ambiguity due the ambiguous nature of the range determined by the transmitted pulses and the echo received. Table 1.1 summaries the various Range/Doppler ambiguity relationships. According to the PRF value of the waveform, it is classified as Low-, Medium- or High-PRF depending on the targets of interest, the carrier wavelength, the detectable range, and the nature of the clutter.

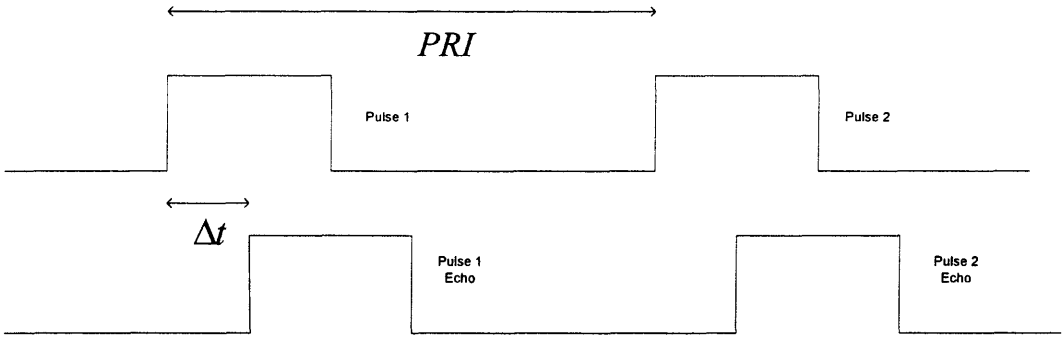

Figure 1.1 Range Ambiguity.

Table 1.1 Summary of Waveform Ambiguity relationships.

	LOW PRF	MEDIUM PRF	HIGH PRF	CW
RANGE	Unambiguous	Ambiguous	Ambiguous	Ambiguous
DOPPLER	Ambiguous	Ambiguous	Ambiguous	Unambiguous

1.4 Range Resolution

Range resolution of radar tells us the ability of radar to detect distinct objects, which are in close proximity. The radars normally have a minimum a range R_{min} and a maximum range R_{max}. The distance between R_{min} and R_{max} is divided into M range bins, each of width ΔR.

$$M = \frac{R_{max} - R_{min}}{\Delta R} \tag{1.5}$$

If two targets are separated by at least ΔR, they are resolved in range as shown in the Figure 1.2. Targets within the same range bin cannot be separated. Most of the radar designers try to minimize ΔR to get better range resolution and detect targets that are closer to each other. Reduction in ΔR can be achieved by using phase codes, which will be discussed in the next chapter.

$$\Delta R = \frac{c\tau}{2} = \frac{c}{2B} \tag{1.6}$$

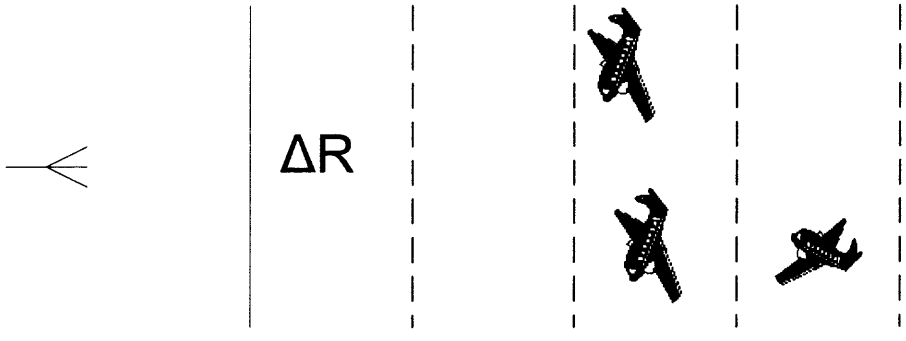

Figure 1.2 Range Resolutions.

As can be seen, the pulse width has to be made as small as possible for better range resolution and detecting targets that are close to each other. But as the pulse width is

reduced, the average power transmitted becomes small. Hence to have a trade off, other types of waveforms are used such as pulse compression techniques.

1.5 Doppler Resolution

Doppler frequency tells weather a target is moving or stationary. The Doppler causes a shift in the central frequency of the incident waveform. The frequency shift may be either positive or negative depending on the motion of the target. It is used to find the velocity of the target.

The Doppler frequency shift is the difference between the received frequency and the transmitted frequency. The Doppler resolution of a target is limited to $\frac{1}{pulsewidth}$.

The Doppler shift is defined as the shift in the transmitted frequency due to the motion of the object. The Doppler shift is the difference between the received and transmitted frequency. If the difference is positive the target is moving towards the reference and if it is negative the object is moving away from the reference.

$$f_d = f_r - f_t; \tag{1.7}$$

where f_r is the received frequency from the target, f_t is the transmitted frequency and

$$f_d = \frac{2v}{\lambda} \tag{1.8}$$

v is the velocity with which the target is moving and λ is the wavelength of the transmitted signal.

1.6 Swerling Models

Dr. Peter Swerling [2] modeled complex targets with simple scatterers and observed its statistics. He developed four different models of cross-section fluctuations according to the probability density function of the radar cross-section and to the "fluctuation velocity". This work was first analyzed by Marcum, Swerling extended the work to four distinct cases that account for radar variations in the target cross section. The four cases are Swerling I, Swerling II, Swerling III and Swerling IV. The constant target cross-section case analyzed by Marcum is known as Swerling V or Swerling 0.

Swerling Case 1: The echo pulses received from target on any one scan are of constant amplitude throughout the entire scan, but are independent from scan to scan. The probability density function for the cross section σ is given by Equation (1.9)

$$p(\sigma) = \frac{1}{\sigma_{av}} \exp\left(-\frac{\sigma}{\sigma_{av}}\right) \qquad \sigma > 0 \tag{1.9}$$

σ_{av} is the average value of target cross section. This case is for many independent target scatters.

Swerling Case 2: The Probability density function is same as Case 1, but fluctuations are independent from pulse to pulse rather than scan to scan.

Swerling Case 3: The echo pulses received from target on any one scan are of constant amplitude throughout the entire scan, but are independent from scan to scan. The probability density function for the cross section σ is given by Equation (1.10)

$$p(\sigma) = \frac{4\sigma}{\sigma_{av}^2} \exp\left(-\frac{2\sigma}{\sigma_{av}}\right) \qquad \sigma > 0 \tag{1.10}$$

This Swerling case represents targets that are modeled as one large scatter and many small scatters.

Swerling Case 4: The Probability density function is same as Case 3, but fluctuations are independent from pulse to pulse rather than scan to scan.

Table 1.2 summaries the Swerling model.

Table 1.2 Swerling Model Summary

Swerling type	Representation	Fluctuation
Swerling I	Many small equal scatters	Scan to scan
Swerling II	Many small equal scatters	Pulse to pulse
Swerling III	One dominant and many small scatters	Scan to scan
Swerling IV	One dominant and many small scatters	Pulse to pulse
Swerling V	Constant Cross section	Constant

CHAPTER 2

AMBIGUITY FUNCTION OF RADAR

2.1 Introduction to Ambiguity Function

The Ambiguity function for Radar Signals was introduced by Woodward in 1953 [22]. It is also known as the uncertainty function, resolution function, two-dimensional autocorrelation function, time frequency autocorrelation function and Woodward ambiguity function. It plays an important role in both the detection and resolution of moving targets.

The Ambiguity function is defined as the absolute value of the envelope of the output of a matched filter. The input signal to the filter is a Doppler shifted version of the return signal, to which the filter is matched. If u(t) is the (complex) envelope of the transmitted signal, then $u^*(t-\tau)\exp(j2\pi\nu t)$ is the Doppler shifted return signal. The ambiguity function is given by Equation (2.1).

$$|X(\tau,\nu)| = \left| \int_{-\infty}^{\infty} u(t)u^*(t-\tau)\exp(j2\pi\nu t)\partial t \right| \tag{2.1}$$

The filter is matched to a signal expected at a nominal center frequency and at a nominal delay. The two parameters of the ambiguity function are delay τ and frequency shift ν [15]. It also describes the interference caused by range and /or Doppler of a target when compared to a reference target of equal RCS (Radar Cross Section).

2.2 Interpretation of Ambiguity Diagram

The ambiguity surface shows the output of the matched filter for a stationary or moving target, range and Doppler resolution, as well as sidelobe structure in the Delay-Doppler

plane. The Ambiguity function gives an idea of the location of the target. It also tells us the performance of a particular modulation and code used for transmission in detecting the targets characteristics.

The three dimensional picture of the Ambiguity function gives an idea of the behavior of the main lobe, which is compared to the sidelobes. The mainlobe is the return from the target. The sidelobe arises due to the self clutter, interference and autocorrelation properties of the waveform. The sidelobes are undesirable since they can obscure other targets.

The ideal Ambiguity function is a spike of infinitesimally small width and peaking at zero. Such an ambiguity function provides perfect resolution between neighboring targets. Unfortunately such an ambiguity function cannot physically exist, because peak should have energy of $(2E)^2$ and a finite volume of $(2E)^2$. Hence, such a thing is not physically possible.

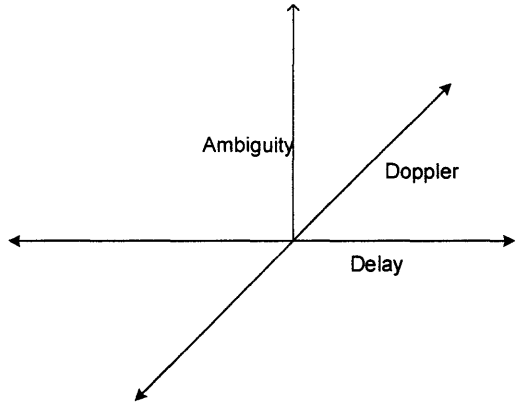

Figure 2.1 Ideal Ambiguity Function

Many ingenious radar waveform design techniques are used, trying to achieve the ideal ambiguity function. The techniques used are mainly to dampen the sidelobes. Several literatures have proposed methods varying from waveform design types to using

mismatched filters. Complementary codes are one of the novel methods, which completely eliminate the sidelobe. Details about complementary codes are elaborated in the following sections. Using mismatched filters to reduce the sidelobes is another technique. Though a small penalty is paid in main lobe reduction (about 3db), it reduces the sidelobes considerably.

2.3 Ambiguity Function of Radar Waveforms

Depending on the use of radar, different types of waveform modulation are used in a radar, mainly analog modulation and pulse modulation. As explained in Chapter-1, analog modulated waveforms give good Doppler resolution and pulse modulated waveforms give good range resolution.

The Primary reason for using different modulation techniques and pulse compression codes is to suppress the sidelobes at the output of matched filter. This phenomenon is called the self-clutter and results in unsatisfactory performance since low-level signals can be masked by the sidelobes of high-level signals. The following section talks about different techniques used to suppress self-clutter and the plot of their ambiguity function

2.3.1 Single Pulse Ambiguity Function

The Single pulse is one of the simplest functions to plot the ambiguity diagram. It gives an understanding of the range and Doppler resolution of the pulse.

The single pulse is given by Equation (2.2)

$$u(t) = \frac{1}{\sqrt{t_p}} rect \frac{t}{t_p} \tag{2.2}$$

where t_p is the duration of the pulse. The mathematical expression for the Ambiguity function for a single pulse is given by,

$$X(\tau,\nu) = \left| \left(1 - \frac{|\tau|}{t_p}\right) \frac{\sin\left[\pi t_p (1 - |\tau|/t_p)\nu\right]}{\pi t_p (1 - |\tau|/t_p)\nu} \right| \qquad |\tau| < t_p \tag{2.3}$$

where t_p is the delay, τ is the time axis and f_d is the Doppler.

Figure 2.2 shows the three-dimensional plot of an ambiguity function for a single pulse

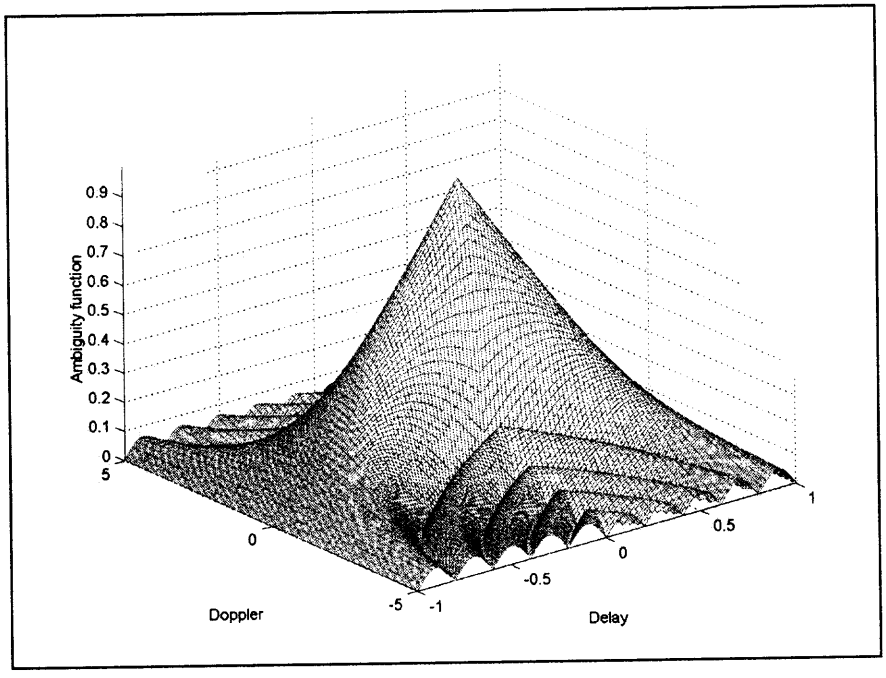

Figure 2.2 Single Pulse 3-D Ambiguity function

The three axis are Doppler, Delay and magnitude of the ambiguity function. The Delay can be obtained by setting Doppler $\nu = 0$, yielding

$$|X(\tau,0)| = 1 - \frac{|\tau|}{t_p} \tag{2.4}$$

The plot of the same is shown in figure 2.3. It can be seen that the Delay cut is similar to the autocorrelation of the sequence. As we know, the autocorrelation of a rectangular function is a triangular function.

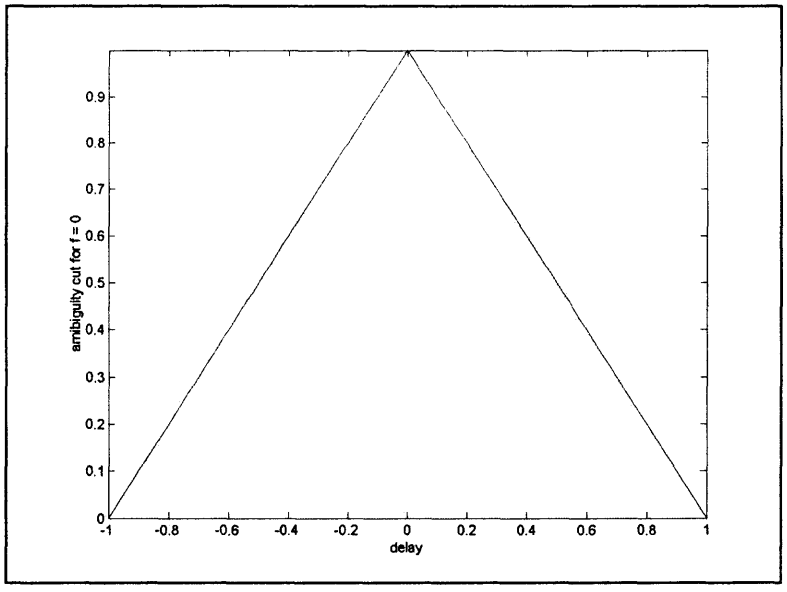

Figure 2.3 Single Pulse Ambiguity function along delay axis

Similarly the cut along the Doppler axis is obtained by setting $\tau = 0$ yielding

$$|X(0,\nu)| = \left|\frac{\sin(\pi t_p \vartheta}{\pi t_p \nu}\right| \tag{2.5}$$

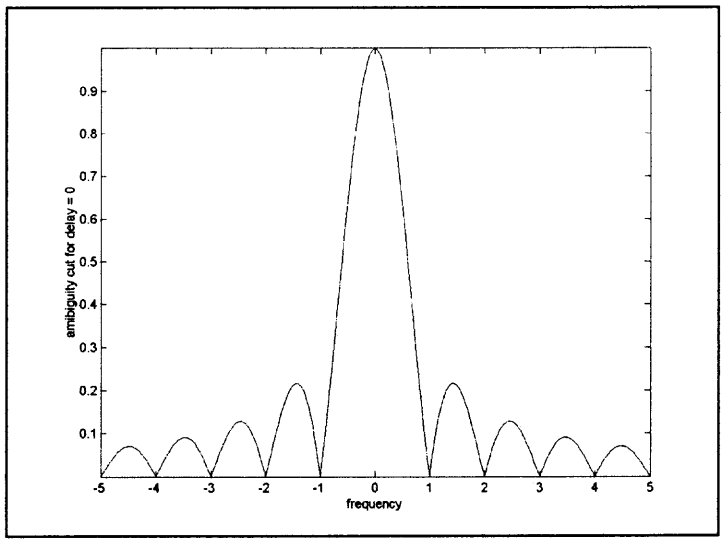

Figure 2.4 Single pulse Ambiguity function along Doppler axis

The single pulse is used in the simulation of MIMO radar in chapter 4. The single pulse transmitted sees a fading channel and in the other scenario they see a non-fading channel. When the single pulse sees a non-fading channel, it's the ideal case or Swerling 5 model. These two scenarios form the boundaries for the performance of MIMO radar.

2.3.2 Linear Frequency Modulation Ambiguity Function

To get better resolution in the ambiguity function we use Linear Frequency Modulation (LFM) pulse. LFM pulse is widely used pulse compression signal, because it is easy to generate, insensitive to Doppler shifts and has many ways to generate the signal.

A LFM complex envelope signal is defined as

$$u(t) = \frac{1}{\sqrt{t_p}} rect\left(\frac{t}{t_p}\right) \exp(j\pi kt^2) \tag{2.6}$$

The ambiguity of a LFM wave is given by Equation (2.7). Figure 2.5 is a plot of the ambiguity function.

$$|X(\tau,\nu)| = \left| \left(1 - \frac{|\tau|}{t_p}\right) \frac{\sin[\pi t_p (1-|\tau|/t_p)(\nu + k\tau)]}{\pi t_p (1-|\tau|/t_p)(\nu + k\tau)} \right| \tag{2.7}$$

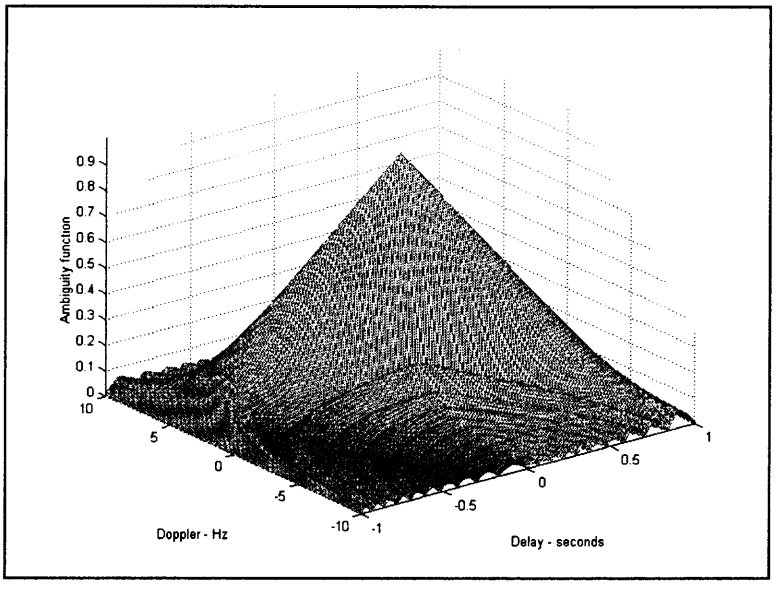

Figure 2.5 The LFM chirp 3-D Ambiguity function

The zero Doppler cut is obtained by setting $\nu = 0$, yielding

$$|\mathrm{X}(\tau,0)| = \left| (1-|\tau|/\tau_p) \frac{\sin[\pi k \tau t_p (1-|\tau|/t_p)]}{\pi k \tau t_p (1-|\tau|/t_p)} \right| \qquad |\tau| \le t_p \tag{2.8}$$

Figure 2.6 is the zero Doppler plot of the LFM chirp ambiguity function. It can be observed that the sidelobes are reduced compared to a single pulse case. This is one of the main advantages of using LFM chirp.

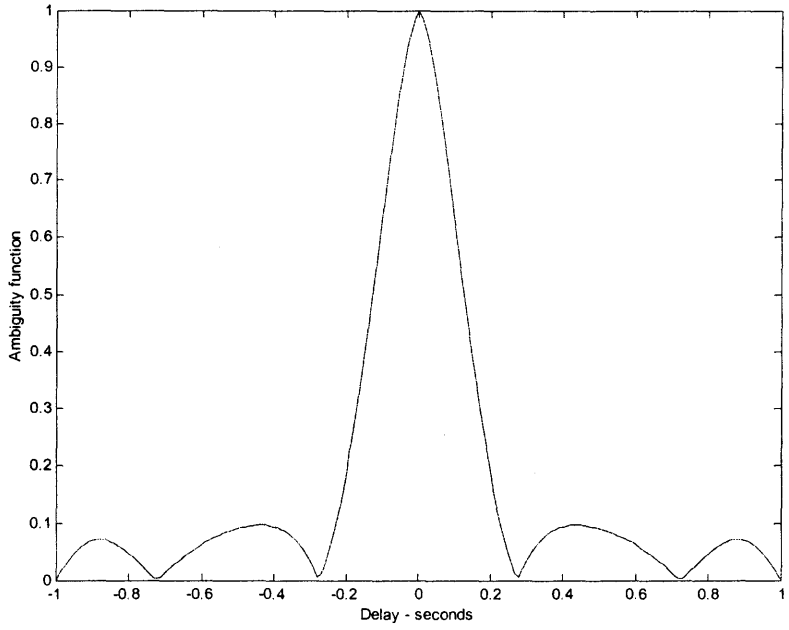

Figure 2.6 LFM chirp zero Doppler

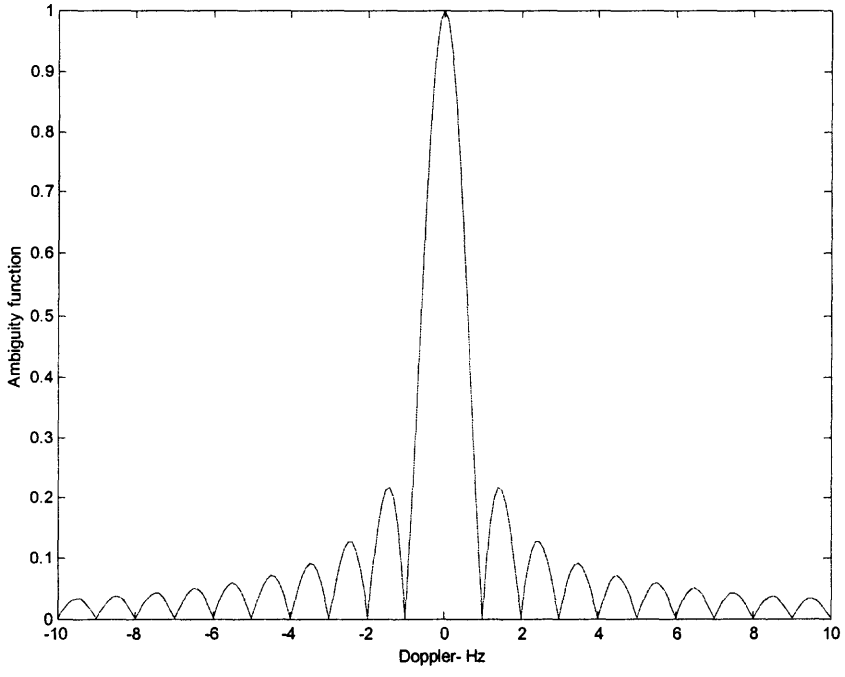

Figure 2.7 LFM chirp zero Delay

When the target is moving very fast, the de-correlation time may be very short. Due to this, the Doppler resolution becomes bad. In addition, the shape of the radars response is determined by the Ambiguity function of the waveform transmitted. In LFM modulation, there are many ways to improve this resolution. One such case was presented in [9]. The paper uses two LFM modulated waves and combines them by multiplying the two waves. Due to this, it is shown that there is a better resolution of the target, but extra processing is involved.

2.3.3 Ambiguity Function of Phase Codes

In this section we discuss about Phase Coding. This is a digital coding technique, in Phase coding; the envelope is constructed from contiguous pulses of constant amplitude. The modulation is on the phase of each pulse. The complex envelope of the phase-coded signal is give by Equation (2.9)

$$u(t) = \sum_{k=0}^{K-1} u_k(t - kT) \tag{2.9}$$

$$u_n(t) = \exp(j\theta_n) \qquad 0 \le t \le T \tag{2.10}$$

Here we discuss about Barker codes, Pseudo Random codes like gold codes and the Complementary codes.

2.3.3.1 Barker Codes. Barker codes are binary phase coding sequences of length R, which result in ambiguity functions with side lobe levels at zero Doppler not higher than 1/R. These codes have phase jumps of 180 or 0 degrees. Only nine such sequences are known. The longest one has a length of R = 13. The nine sequences are listed in Table 2.1

Table 2.1 Barker Codes

Code length	Code Elements	Side Lobe Reduction (db)
2	1 -1	6
	1 1	
3	1 1 -1	9.5
4	1 1 -1 1	12.0
	1 1 1 -1	
5	1 1 1 1 -1 1	14.0
7	1 1 1 -1 -1 1 -1	16.9
11	1 1 1 -1 -1 -1 1 -1 -1 1 -1	20.8
13	1 1 1 1 1 -1 -1 1 1 -1 1 -1 1	22.3

Only codes of length 2 and 4 are known to have 2 sequences; all others have only a single sequence for one code. Figure 2.8 is a three dimensional plot of Ambiguity function of Barker code of length 13. It can be observed from the Figure that the main lobe is $2R\Delta\tau$ wide and the peak value is R. There are (R-1)/2 side lobes on either side of the main lobe.

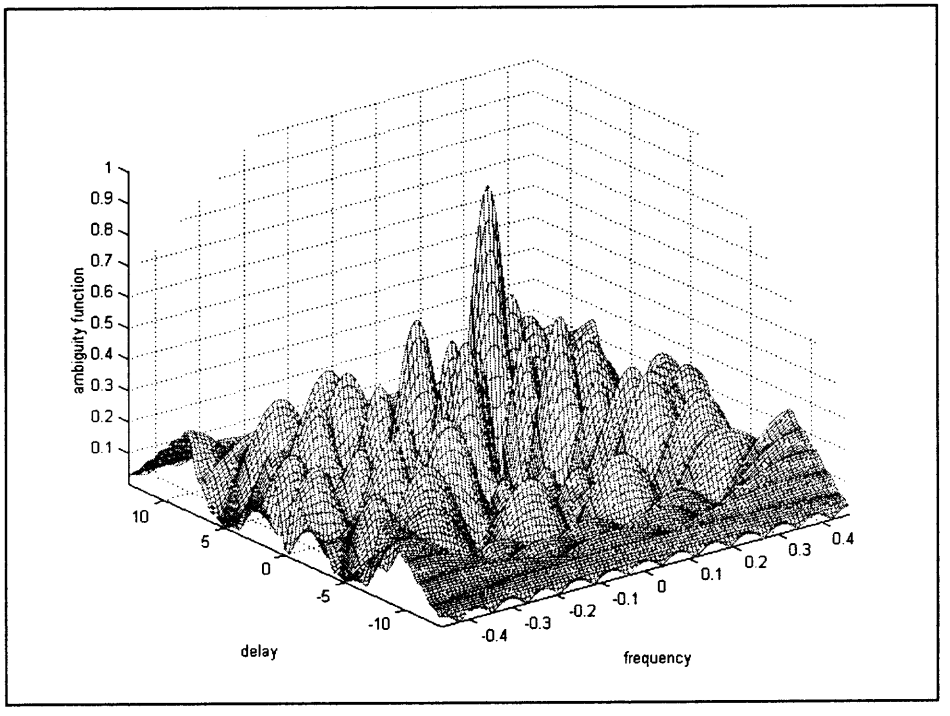

Figure 2.8 Ambiguity function for Barker code of Length 13

Figure 2.9 is a zero Doppler plot. It can be observed from the Figure that the maximum side lobe reduction is offered by a Barker code of length 13, which is -2.3db.

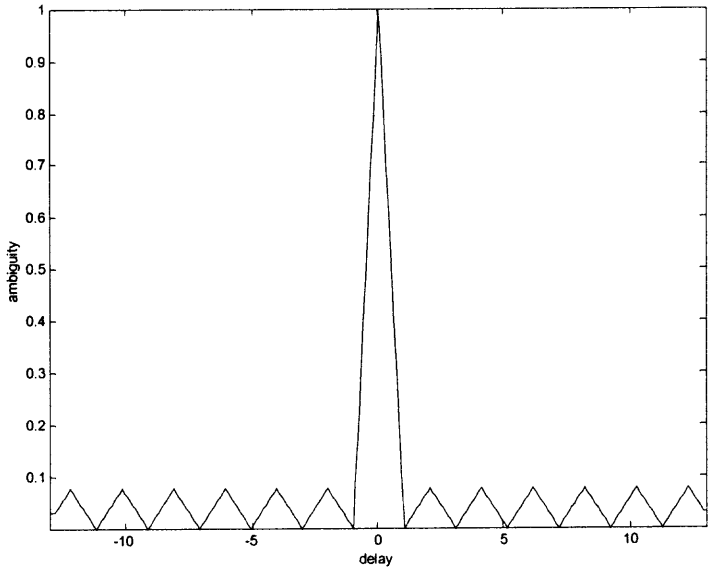

Figure 2.9 Zero Doppler cut for Barker Code of Length 13

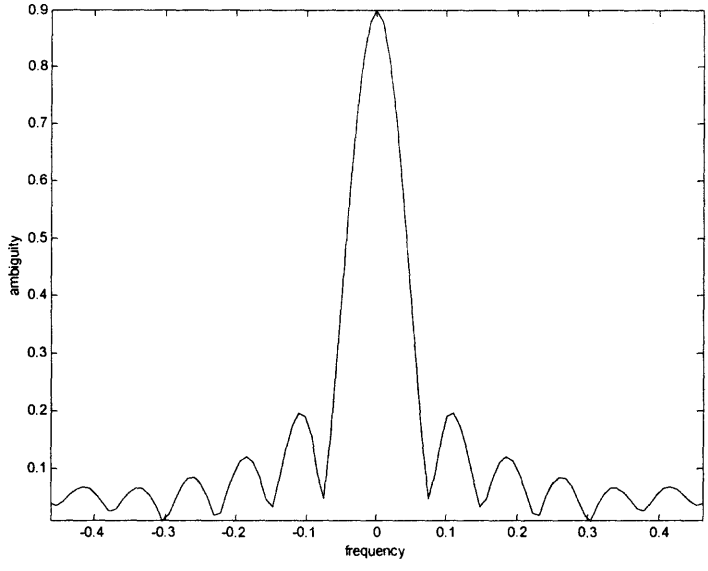

Figure 2.10 Zero Delay cut for Barker Code of length 13

Barker codes greater than length 13 have not yet been found; so some non-optimal solutions like combining Barker codes have been suggested in the literature. The maximum length of a combined Barker code is of length R = 13x13 = 169. These codes would have been ideal codes to be used in MIMO Radar, but since only a few codes are known, they are not useful. Hence pseudo random codes like gold codes are used, which is explained in the following section.

2.3.3.2 Gold Code Sequences. During the early radar years, pulse compression was done using Linear frequency Modulation (LFM) but these waveforms had range recurrent sidelobe levels, which degrade as the number of distinctly coded pulses increase for a constant compression ratio [18]. The disadvantage prompted research into maximal length pseudo noise sequences. Gold codes, which are a subset of the pseudo noise sequences, are having a distinct advantage over other sequences. These codes have low

cross correlation properties and the sidelobes are also small compared to the main lobe. There is also no significant degradation as the number of pulses coded is increased.

They offer well-controlled cross-correlation properties, essentially manageable interference between successive pulses when used for pulse compression radars. Figure 2.11 illustrates the 3-D plot of gold code ambiguity function.

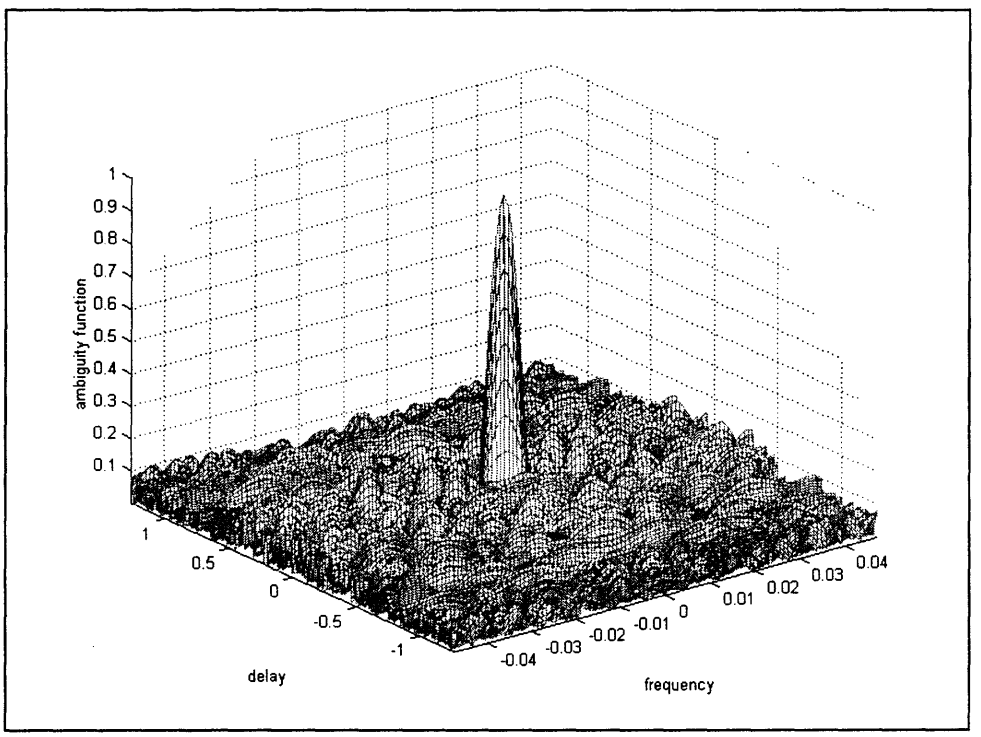

Figure 2.11 Ambiguity Function of Goldcode

It can be observed from Figure 2.12 that the main lobe amplitude has increased considerably. The main lobe to sidelobe ratio can be further increased by increasing the number of chips in a pulse. Various criteria have been proposed to get optimal gold codes, which is further elaborated in Chapter 4. Since gold codes have good cross correlation properties they are used as MIMO transmitter waveform.

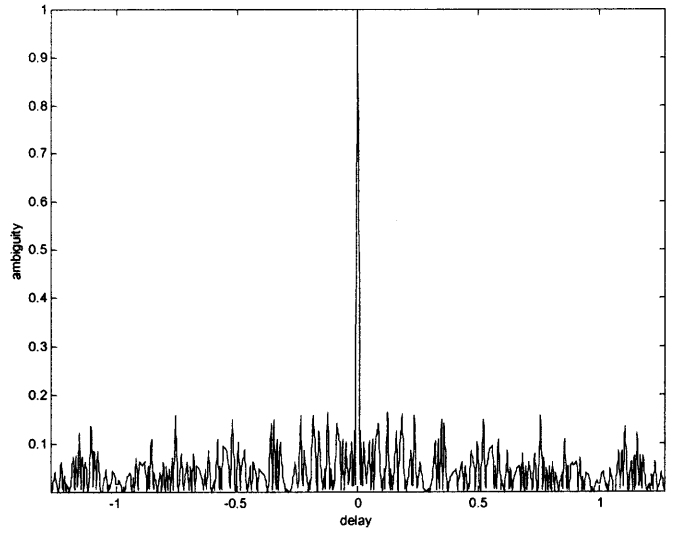

Figure 2.12 Zero Doppler cut of Goldcode Ambiguity function

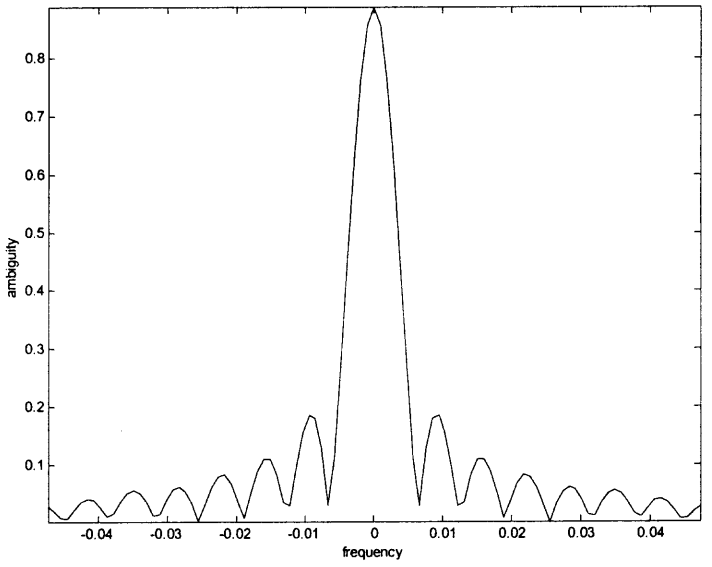

Figure 2.13 Zero Delay cut of Goldcode Ambiguity function

2.3.3.3 Complementary Codes. A complementary code pair, as defined by Golay, consists of two equal length sequences with the property that the algebraic sum of the Autocorrelation of the sequences is zero except for only one sample point [11]. Golay pairs are available for lengths of L.2k, where the k is any integer 0,1,2,3, ... and L is the kernel length. It may be noted that only kernels of 2,10 and 26 were discovered [17]. Hence Multiphase Complementary codes were introduced. These codes are constant in amplitude and have phase parameters. MPC codes of lengths L = 2, 3, 10, 26 can be recursively expanded for lengths of $L.2^k$. Considering a MPC codes $[S_{L+1}]$ and $[C_{L+1}]$ of lengths (L+1)

$$[S_{L+1}] = [s_0, s_1, \ldots\ldots\ldots\ldots s_l] \tag{2.11}$$

Each element of the code S is given by

$$s_l = A(t - l\tau_s)e^{j(w_o t + \phi_l)} \tag{2.12}$$

where A(t) is the amplitude. The zero Doppler autocorrelation function of S is given by

$$\chi(\tau) = \sum_{l=0}^{L+1-\tau} s_l . s_{l+\tau}^{*} \qquad \tau > 0 \tag{2.13}$$

Similarly the Complementary sequence $[C_{L+1}]$

$$[C_{L+1}] = [c_0, c_1, \ldots\ldots\ldots\ldots c_l] \tag{2.14}$$

Each element is given by

$$c_l = A(t - l\tau_s)e^{j(w_o t + \theta_l)} \tag{2.15}$$

and the autocorrelation function is given by equation 2.16

$$\psi(\tau) = \sum_{l=0}^{L+1-\tau} c_l . c_{l+\tau}^{*} \qquad \tau > 0 \tag{2.16}$$

The sequences are MPC if the sum of autocorrelation satisfies equation 2.17

$$\chi(\tau) + \psi(\tau) = \begin{cases} 0 & \text{for all } \tau > 0 \\ 2(L+1) & \text{for } \tau = 0 \end{cases} \tag{2.17}$$

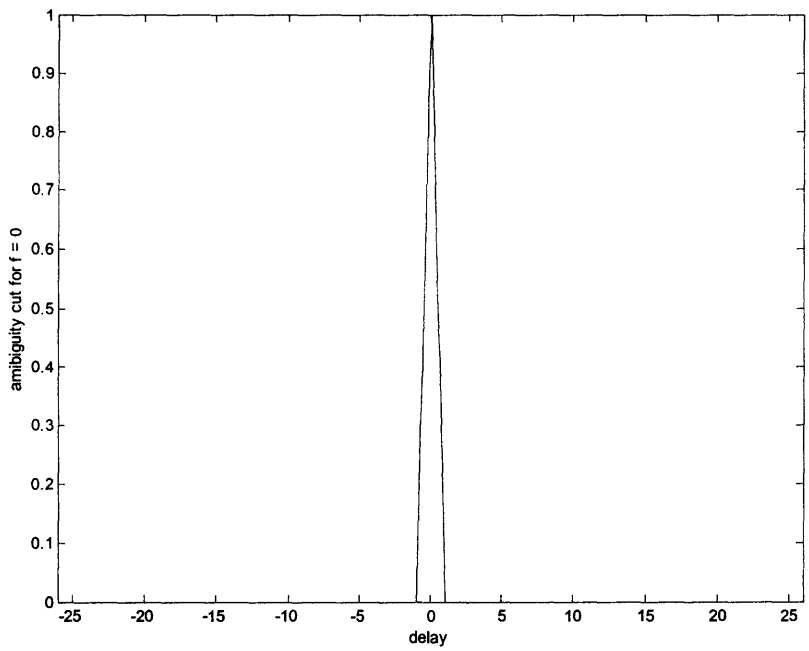

Figure 2.14 Zero Doppler Ambiguity function for MPC code of length 26

It can be observed from Figure 2.14 that there are no sidelobes. These are the only known codes that try to achieve ideal ambiguity function as explained in the beginning of the chapter.

2.4 Measurements used for Evaluating the Ambiguity Function

In radar literature two measurements are mainly used to measure the effectiveness of an ambiguity function. These are namely PSLR (Peak Sidelobe Ratio) and ISLR(Integrated Sidelobe Ratio). Apart from these, there are several other measurements to quantify the ambiguity function like the Main lobe width measurement. The following section gives a brief introduction to them.

The PSLR indicates the ability of the radar to detect weak targets. It is the ratio of the largest sidelobe value (outside the specified mainlobe region) to the mainlobe peak. It is associated with the probability of a false alarm in a particular range bin due to the presence of a target in a neighboring range bin.

$$PSLR(db) = 20\log\frac{|l\arg est\_sidelobe|}{|manilobe\_peak|} \tag{2.18}$$

The ISLR is a measure of how much energy is leaking from the mainlobe of the impulse response function of the target. It is a measure of the energy distributed in the sidelobes. It is important in dense target scenarios and when distributed clutter is present. It is the integrated sidelobe to mainlobe power ratio.

$$ISLR(db) = 10\log\frac{\sum(sidelobe)^2}{(mainlobe\_peak)^2} \tag{2.19}$$

Main lobe width measurement is used to measure the main lobe of the ambiguity function although not used and referred in many literatures. It is highly desirable to have the main lobe width as small as possible to precisely locate the target. As will be seen in the next chapter the main lobe width can be kept small by using phase coding with gold codes and the width decreases as the number of gold code chips in a pulse increases.

CHAPTER 3

MULTIPLE INPUT MULTIPLE OUTPUT RADAR

3.1 Multiple Input Multiple Output Communication Systems

Multiple-input multiple-output (MIMO) communication techniques have been an important area of research for next-generation wireless systems because of their potential for high capacity, increased diversity, and interference suppression. This technique is based on the theoretical work done by Teletar and Foschini. This technology received a boost when Tarokh et al. and Alamouti introduced space-time coding techniques to improve performance based on diversity.

MIMO systems have multiple transmitters and multiple receivers. By increasing the number of transmitter/receiver antennas, MIMO systems are able to take advantage of a rich scattering channel to drastically increase the overall transmission capacity. In other words instead of trying to mitigate the fading channel, which has been a problem in traditional wireless communication systems, MIMO exploit the multi-path to increase throughput. This benefit comes at an expense in the complexity of the hardware, but not at the cost of signal spectrum or power. MIMO communication systems overcome the problems caused by fading by transmitting different streams of information from several de-correlated transmitters. Since the transmitters are de-correlated different channels undergo independent fading. Basically MIMO systems offer diversity and multiplexing gain.

Diversity gain means receiving a signal transmitted through several different independent fading channels, then the probability that at least one of the channels is not in a deep fade is high. The probability increases when the number of channels is

increased. The three main forms of diversity exploited in wireless communication are temporal diversity, frequency diversity and spatial diversity.

Temporal diversity is applicable in a channel that has time selective fading. In this case replicas of the transmitted signal are provided across time by a combination of channel coding and time interleaving strategies. The main requirement is that the channel must provide sufficient variations in time.

Frequency diversity is effective when the fading is frequency selective. This type of diversity provides replicas of the original signal in the frequency domain. This is applicable is cases where the coherence bandwidth of the channel is small compared with the bandwidth of the signal.

In spatial diversity the signals are transmitted or received from antennas that are spaced by more than the coherence distance apart. In this case replicas of the same signal are provided across different antennas of the receiver. The transmit signals from the antennas are spaced more than the coherence distance apart. The coherence distance is the minimum spatial separation of antennas for independent fading and depends on the angle spread of the multi-paths arriving at or departing from the antenna array. Spatial diversity can be categorized as Receiver diversity and Transmit diversity.

In transmit diversity the channel information is needed to exploit appropriate signal processing techniques at the receiver. Transmit diversity requires sophisticated methods like Space time codes when the channel information is not known. Space time coding which uses coding across different transmitters and time to send signals that can be combined at the receiver to obtain diversity. Receiver diversity merely needs multiple

antennas that fade independently and receive diversity provides array gain. Maximal ratio combining is applied to improve signal quality at the receivers.

MIMO communication has several applications in cellular networks and wireless LANs. High capacity is achievable by such systems with space-division multiplexing. Wireless LANs seem to be a natural fit for MIMO because of the rich multi-path present indoors. Currently many WLAN routers are available in the market with MIMO technology.

3.2 MIMO Radar

A MlMO radar is defined as any radar that probes a channel by transmitting multiple signals (separated temporally, spectrally, or spatially) and received with some similar multiplicity [6].

MIMO Radar exploits the independence between signals at array elements. In conventional radar, target scintillations are regarded as a nuisance parameter that degrades radar performance. MIMO radar capitalizes on target scintillations to improve the radar performance. The MIMO radar system under consideration consists of a transmit array with widely spaced elements such that each views a different aspect of the target [8], and work has been done in MIMO direction finding. In [7] MIMO radar focuses on direction finding and ignoring the range and Doppler effects. This thesis focuses on range resolution by analyzing the ambiguity function.

In MIMO radar, each transmitter transmits a waveform with a different code. The waveform illuminates the target, and reaches the receiver where it is filtered. Each of the waveform is reflected over different aspects of the target. At the receiver thermal noise is

added to the received waveform. MIMO radar greatly improves detection and estimation performance as it helps to overcome target fades. This improvement is generally known as diversity gain. In statistical MIMO [7] radar, the spacing between the array elements is very large. It overcomes target RCS fluctuations by averaging over many de-correlated channels between transmit and receive antennas. MIMO spatial diversity also eliminates the deep interference nulls in the elevation coverage due to surface multi-path reflection.

Radars have to operate in the presence of noise, clutter and other interferences to select the target. This presents a challenging issue for the radar stability, isolation and other hardware related specifications. Radar design is further strained by requirements on fast search rates and high resolution in Doppler and angle. To partially address this problem, radar array Digital Beam Forming (DBF) is used [6]. Specifically these look in one narrow section at a time and perform a single radar function. The advantage of MIMO radar is that the user can lower the peak power transmitted. This MIMO time-energy management technique eases radar equipment specifications and can offer improved performance [6].

In the MIMO radar [6], the author uses Swerling I model with M transmitters and N receivers. The transmitter and receiver are not necessarily collocated. The target is hit by radar waveforms from M transmitter antennas and the reflections are collected by the N receiver antennas. Each target is assumed to be zero mean, unit variance, independent, identically distributed random variables. The signal impinges on the Q targets at angles of $\theta_{m,q}$. Here for evaluating the ambiguity function M transmitters and a single receiver are considered. The Q elements of a single complex target are assumed to be zero mean, unit

variance, independent and identically distributed Gaussian complex variables. The target model is given by Equation (3.1) where ς_Q is the random variable.

$$\sum = \frac{1}{\sqrt{2Q}} \begin{pmatrix} \varsigma_0 & \cdots & 0 \\ \vdots & \ddots & \vdots \\ 0 & \cdots & \varsigma_{Q-1} \end{pmatrix} \tag{3.1}$$

Each of the signals transmitted by M transmitters impinges on the Q elements of the target at angles $\phi_{m,q}$.

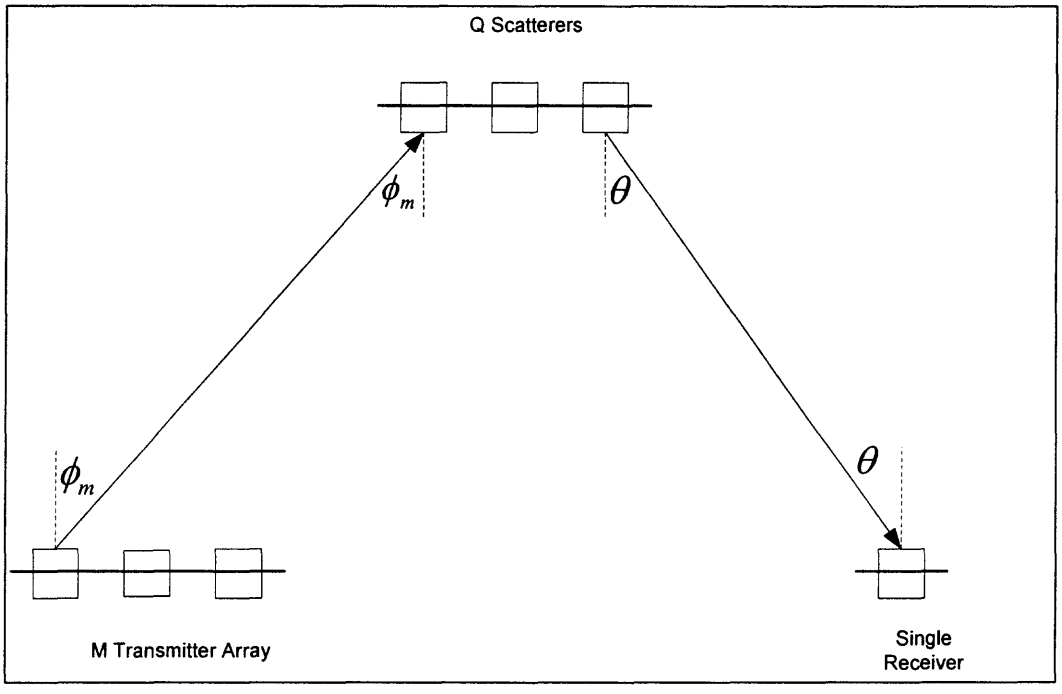

Figure 3.1 Target consisting of multiple scatters.

The signal transmitted by the m[th] transmitter is given by Equation (3,2)

$$g_m = [1, e^{-j2\pi \sin\phi_{m,2}\Delta_2/\lambda}, \ldots\ldots\ldots\ldots, e^{-j2\pi \sin\phi_{m,Q}\Delta_Q/\lambda}]^T \tag{3.2}$$

where Δ_Q is the spacing between signals. The total transmitted signal vectors can now be organized in the M X Q transmit matrix. Since the targets are uniformly spaced $\Delta_q = q.\Delta$.

$$G = [g_1, g_2 \ldots\ldots g_m]^T \tag{3.3}$$

The vector k(θ) given in Equation (3.4) gives the relative phase shift of the signals reflected by the scatters.

$$k(\theta) = [1, e^{j2\pi \sin\theta\Delta/\lambda}, \ldots\ldots\ldots\ldots, e^{-j2\pi \sin\theta(Q-1)\Delta/\lambda}]^T \tag{3.4}$$

The signal received from the mth transmitter is given by Equation (3.5)

$$r_m^{'} = k^T(\theta)\sum g_m s_m \tag{3.5}$$

The transmitted signals is given by the vector s = [s_0,.....,s_{M-1}]. In MIMO it is attempted to exploit the spatial diversity; so it is required that each transmitter sees uncorrelated aspects of the target. Then the received signal components due to the mth transmitter is given by Equation (3.6)

$$r_m^{'} = \frac{1}{\sqrt{2}}\alpha_m s_m \tag{3.6}$$

where α_m is the target fading constant and is given by $\alpha_m = \sqrt{2}1_Q^T \sum g_m$. The fading constants are zero mean and independent, hence $E\{\alpha_m^* \alpha_{m+1}\} = 0$ which leads to Equation (3.7)

$$E\{\alpha_m^* \alpha_{m+1}\} = \frac{1}{2Q} g_m^H 1_Q g_{m+1} = 0 \tag{3.7}$$

Thus the fading constants for different transmitters are uncorrelated if the columns of G are orthogonal.

$$g_m^H g_{m+1} = \sum_{q=0}^{Q-1} e^{j2\pi[(\sin\phi_{m+1} - \sin\phi_m)q\Delta/\lambda]} = 0 \tag{3.8}$$

The received signal vector is given by Equation (3.9)

$$r = K\sum Gs + v = Hs + v \tag{3.9}$$

where v represents the Gaussian noise at the receiver, K represents the propagation paths from the scatters, H incorporates the paths from all the transmitters to the receiver.

3.3 Space Time Codes

Space Time Coding is when the signal is transmitted in space and time i.e. transmitting a signal from different antennas at different time intervals. Alamouti proposed a scheme in which signals where transmitted from two antennas and in two different time intervals. In an Alamouti scheme the encoder takes a block of two symbols and encodes them according to the coding matrix

$$s = \begin{bmatrix} s_1 & -s_2^* \\ s_2 & s_1^* \end{bmatrix} \tag{3.10}$$

The first column represents the first transmit period and the second column represents the second transmit interval [14]. This is further illustrated in Figure 3.2

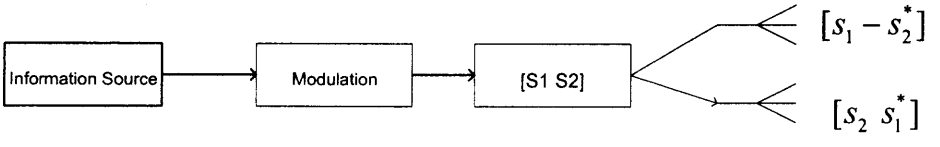

Figure 3.2 Alamouti Space Time Code

The two sequences are orthogonal since the inner product is zero. The received signal are given by r_0 and r_1

$$\begin{aligned} r_0 &= h_0 s_1 + h_1 s_2 + n_0 \\ r_1 &= -h_0 s_2^* + h_1 s_1^* + n_1 \end{aligned} \tag{3.11}$$

where h_0 and h_1 are zero mean, unit variance, independent and identically distributed Gaussian complex variables that denote channel gains between transmit antenna 1 and receive antenna and transmit antenna 2 and the receive antenna, respectively. The noise

samples n_0 and n_1 is also Normal Gaussian zero mean, unit variance, independent and identically distributed. Rewriting in the vector matrix form, the received signal vector r is given by Equation (3.12)

$$r = Hs + n \tag{3.12}$$

where $r = [r_0 \; r_1^*]^T$, $s = [s_0 \; s_1]^T$, $n = [n_0 \; n_1^*]$ and

$$H = \begin{bmatrix} h_0 & h_1 \\ h_1^* & -h_0^* \end{bmatrix} \tag{3.13}$$

is the equivalent channel matrix.

The resulting received signal can be determined using Maximum Ratio Combining.

CHAPTER 4

IMPLEMENTATION AND RESULTS

The proposed scheme of MIMO (Multiple Input Multiple Output) Radar is a novel improvement in Radar performance over conventional radar in detection and estimation of the ambiguity function. In this chapter the ambiguity function is analyzed for gold codes of varying lengths and multiple transmitters in a MIMO environment. The results of Alamouti space-time codes applied to MIMO Radar are also presented. Simulation is carried out for stationary measurements of the target, ignoring Doppler.

4.1 MIMO Radar

The introduction to MIMO Radar is given in Chapter 3. In a MIMO Radar simulation we have multiple transmitters and a single receiver. The transmitted signal illuminates different aspects of the target. At the receiver the received signal and white Gaussian noise are the inputs. The output of each of the Matched Filter is squared and summed, as the fading constants of the different channels are unknown. This is illustrated in Figure 4.1.

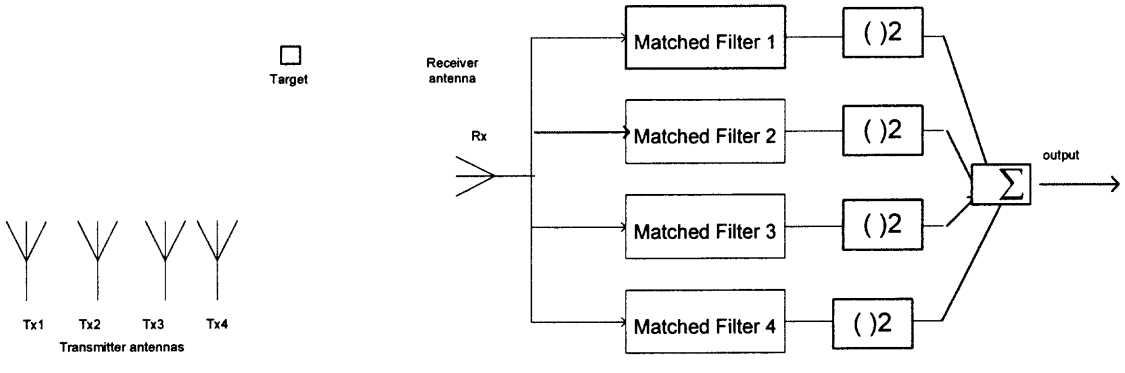

Figure 4.1 MIMO Radar

4.2 Gold Codes

Pseudo-noise (PN) sequences are binary sequences, which exhibit noise like randomness properties. Research of these sequences is primarily motivated for use in spread spectrum communication systems. Gold codes are a special class of Maximal Length (ML) PN sequences and offer well controlled cross correlation properties. The cross correlation properties allow the range recurrent sidelobes of the ambiguity function to remain relatively consistent levels for Gold codes regardless of the number of codes used [18].

Given a preferred pair of sequences of period $n = 2^m-1$, say s= s(t) and r = r(t), we can construct a family of sequences by taking the modulo-2 sum of s with the n cyclic shifted versions of r or vice versa. Thus, we obtain n new periodic sequences with period n. The resulting sequences are called Gold code sequences. Figure 4.1 shows the shift registers for generating a preferred pair of sequences corresponding to the polynomials

$$g_1(x) = x^5 + x^2 + 1 \tag{4.1}$$

$$g_2(x) = x^5 + x^4 + x^2 + x + 1 \tag{4.2}$$

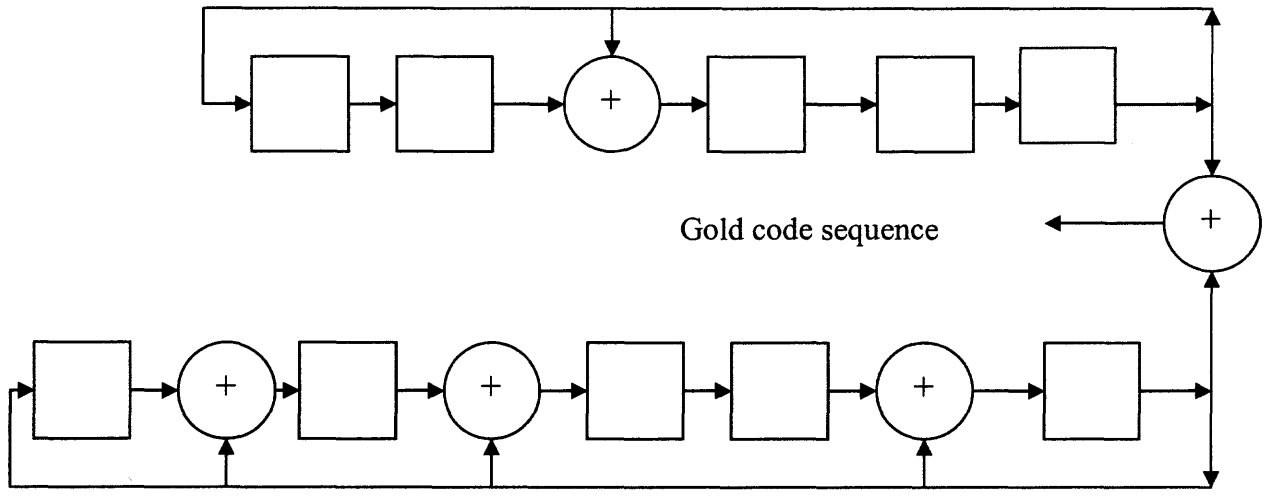

Figure 4.2 Goldcode generation

The cross correlation function for any pair of sequences in the Gold sequences was proven to be three valued with possible values {-1,-t(m),t(m) -2} where

$$t(m) = \begin{cases} 2^{(m+1)/2} + 1 & (odd \quad m) \\ 2^{(m+2)/2} + 1 & (even \quad m) \end{cases} \tag{4.3}$$

The code selection for spread spectrum communication is a very important area. Many publications have been done in this area for finding the optimized codes with least interference. These papers give a good understanding of the different codes and their uses for different optimized criteria. Most of the work is focused on the evaluation of the average interference parameter (AIP) values.

The various criteria are used to optimize the goldcodes are Auto-optimal least sidelobe energy (AO/LSE), Least sidelobe energy auto-optimal (LSE/AO), Maximum sidelobe energy auto-optimal (MSE/AO), Cross optimal minimum mean square cross correlation (CO/MSQCC) and Minimum mean square cross correlation cross optimal

(MSQCC/CO). These properties are explained in [20]. Better Autocorrelation properties can be gained at the expense of worse cross correlation properties. The CO/MSQCC criterion emphasizes the mean square cross correlation parameter instead of the peak correlation in order to reduce the total amount of multiple access interference. Since these optimized codes have low cross correlation, they are selected as phase codes for transmitter.

4.3 MIMO Radar Transmitter Waveform

In designing the waveforms for transmitter the energy per pulse sent out of each transmitter is kept constant regardless of the length of the sequences and the total energy per pulse is kept constant regardless of the number of transmitters.

For a single pulse of duration T_p, the energy per pulse is kept constant.

$$E_p = A^2 T_p \tag{4.4}$$

where E_p is the energy per pulse and A is the amplitude of the pulse and T_p is the duration.

$$A = \sqrt{\frac{E_P}{T_P}} \tag{4.5}$$

At the receiver, the noise gets into the matched filter and is modeled as a white Gaussian noise with variance σ^2.

The noise variance is given by

$$\sigma^2 = \frac{N_0}{2} * \frac{1}{T_P} \tag{4.6}$$

where the noise power spectral density is given by N_o

$$\frac{E_p}{N_0} = \frac{A^2}{2*\sigma^2} \tag{4.7}$$

The plots for $\frac{E_p}{N_0}$ versus PSLR are plotted and compared with multi chip scenario. By doing pulse compression, we are increasing the pulse duration constant and increasing the number of chips per pulse. Since the duration of a chip is constant, the bandwidth remains the same for both a single pulse case and multi chip per pulse waveform.

$$E_p^{'} = E_p \tag{4.8}$$

where E_p is the energy of the single pulse and $E_p^{'}$ is the total energy of the pulse compressed waveform.

$$A^{'2} * N * T_p = A^2 * T_p \tag{4.9}$$

$$A^{'} = \frac{A}{\sqrt{N}} \tag{4.10}$$

The amplitude is reduced by a square root of N where N is the number of chips per pulse. The white noise for a pulse compression waveform is given by $\frac{N_0}{2}$ and is same as single pulse case since the chip duration is same.

$$\frac{E_p}{N_0} = \frac{A^{'2} * N}{2*\sigma^2} \tag{4.11}$$

4.4 Impact of Multiple Transmitters

PSLR is a measurement for ambiguity function, as explained in Chapter 2. The lower the PSLR the better the performance. We explore the MIMO radar by increasing the number of transmit antennas. Each transmit antenna illuminates different aspects of the target.

White Gaussian noise along with the received signal is the input to the matched filter. The PSLR of the ambiguity function is then measured at the output. The main lobe of the ambiguity function follows a Chi Square distribution. Curves for different percentiles are plotted for PSLR vs. $\frac{E_p}{N_0}$. In Figure 1, CO/MSQCC gold codes of length 2047 are used.

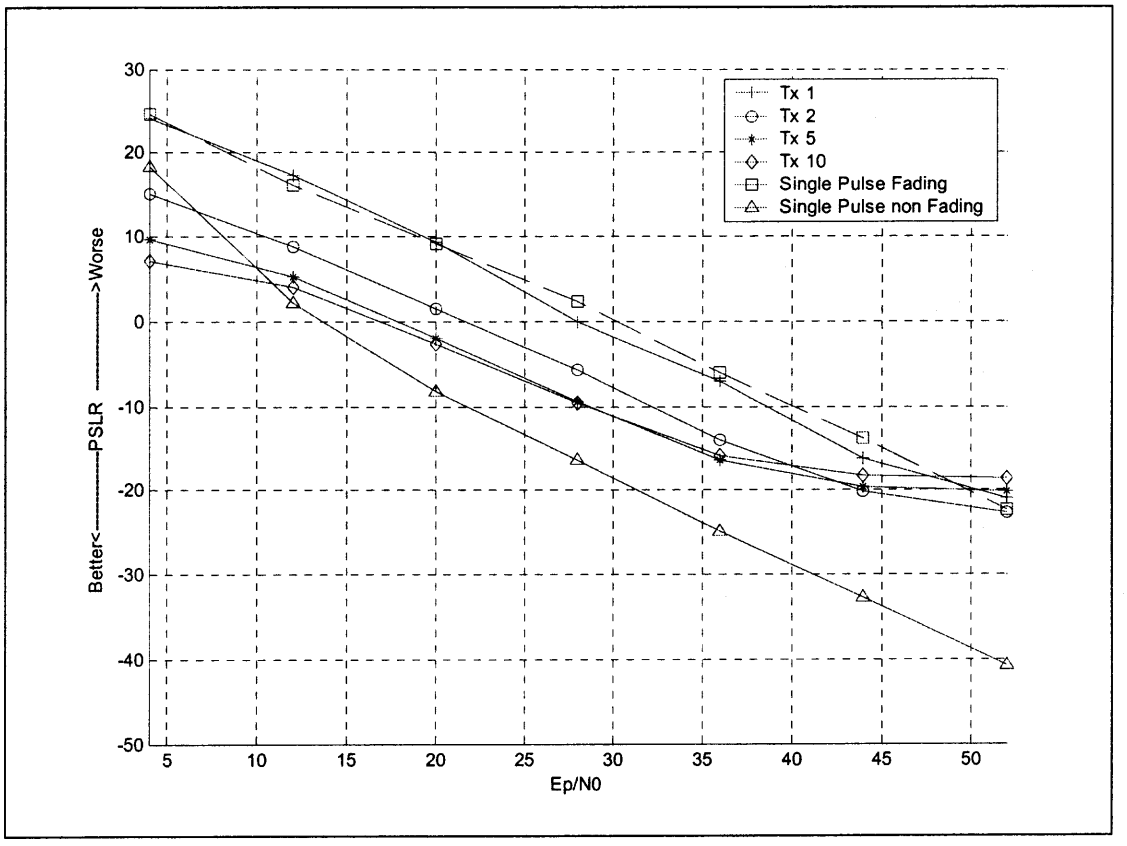

Figure 4.3 Multi Transmitter plot for PSLR at 99 percentile

Figure 4.3 illustrates the 99 percentile. The notation 99% (percentile) implies that 99% of the target realizations the PSLR have a lower and therefore a better value than the plotted one. From Figure 4.3, it is observed that as the number of transmit antennas are increased, the performance is better i.e. the PSLR is lower when $\frac{E_p}{N_0}$ becomes small.

This is due to the diversity gain we get from multiple antennas. The two single pulse cases are like the outermost and innermost boundaries for the simulation. Single pulse without fading is a Swerling 5 model. As can be seen from Figure 4.1, at low $\frac{E_p}{N_0}$, the multiple transmit antenna performs better than a single transmit antenna.

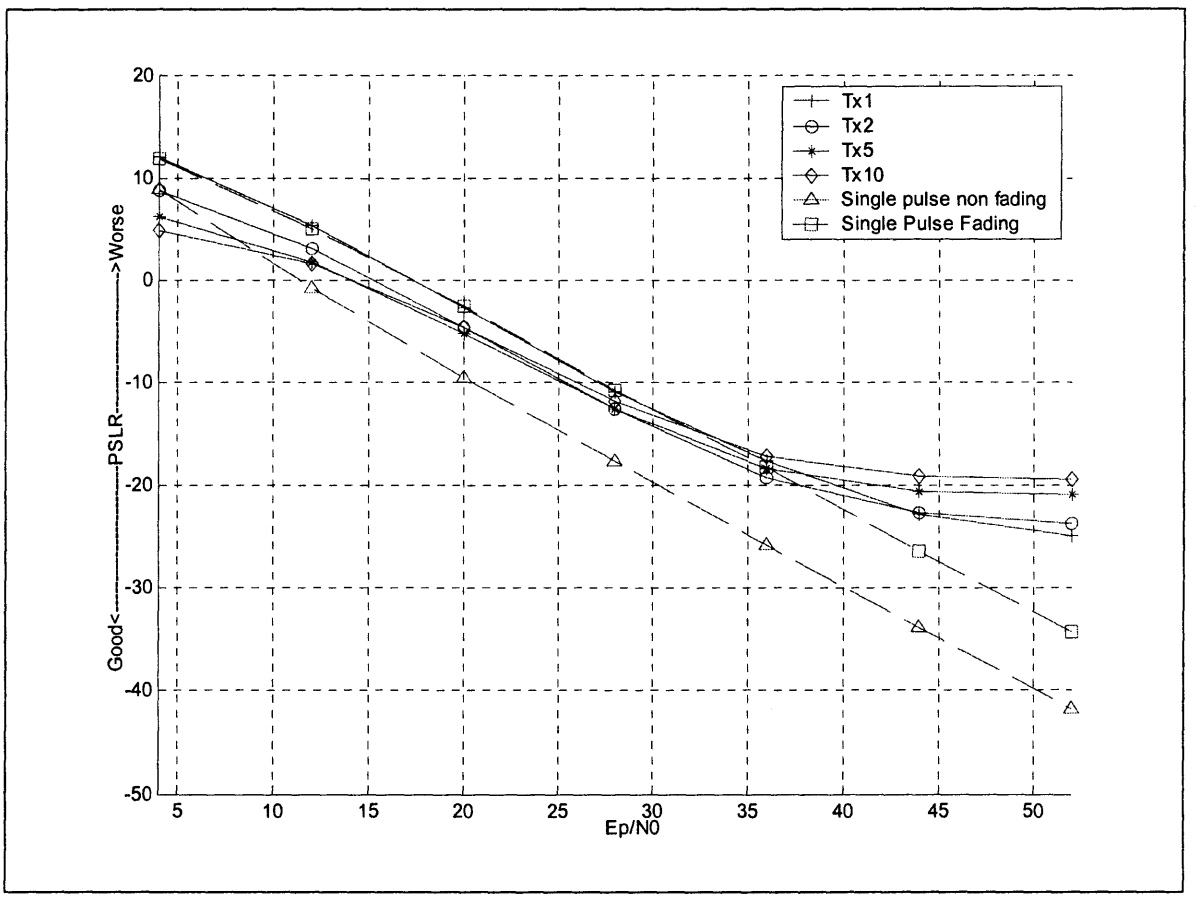

Figure 4.4 Multi Transmitter plot for PSLR at 85 percentile

At high $\frac{E_p}{N_0}$, the mutual interference due to cross correlation additionally affects the performance in multiple transmitters and thus cancels the advantages achieved by

diversity. Since thermal noise is negligible at high $\frac{E_p}{N_0}$, the mutual interference can be approximated as a Gaussian random variable with a variance σ_{MI}^2.

$$\sigma_{MI}^2 = \frac{M}{N} \tag{4.12}$$

where M is the number of Transmit antennas and N is the code length transmitted. Due to the mutual interference, the performance of multiple transmitters is worse than single transmitter in high $\frac{E_p}{N_0}$. For two different transmitter setups, Tx_2 and Tx_{10}, the effect of mutual interference in PSLR in high $\frac{E_p}{N_0}$ can be computed as

Mutual Interference = $10*\log(Tx_2) - 10*\log(Tx_1) = 10*\log(10) - 10*\log(2)$

= 6.87 db

This expectation is verified from the Figure 4.2, which validates the presented results. For low $\frac{E_p}{N_0}$ values increasing the number of transmitters corresponds to approximating a non fading target (Swerling 5). It can be further observed from Figure 4.3 that the PSLR difference between Tx_1 and Tx_{10} for 99 percentile at $\frac{E_p}{N_0}$=25 is approximately 10db, this is verified from Figure 4.5 which is the CDF plot of a Chi square function that the ratio is 13db. The difference between the two results is due to the noise at the receiver. Similarly it can be verifed for the 85 percentile plot from Figure 4.4 we observe the difference between Tx_1 and Tx_{10} is approximately 4 db and from the Figure 4.5 we get a ratio of 7db.

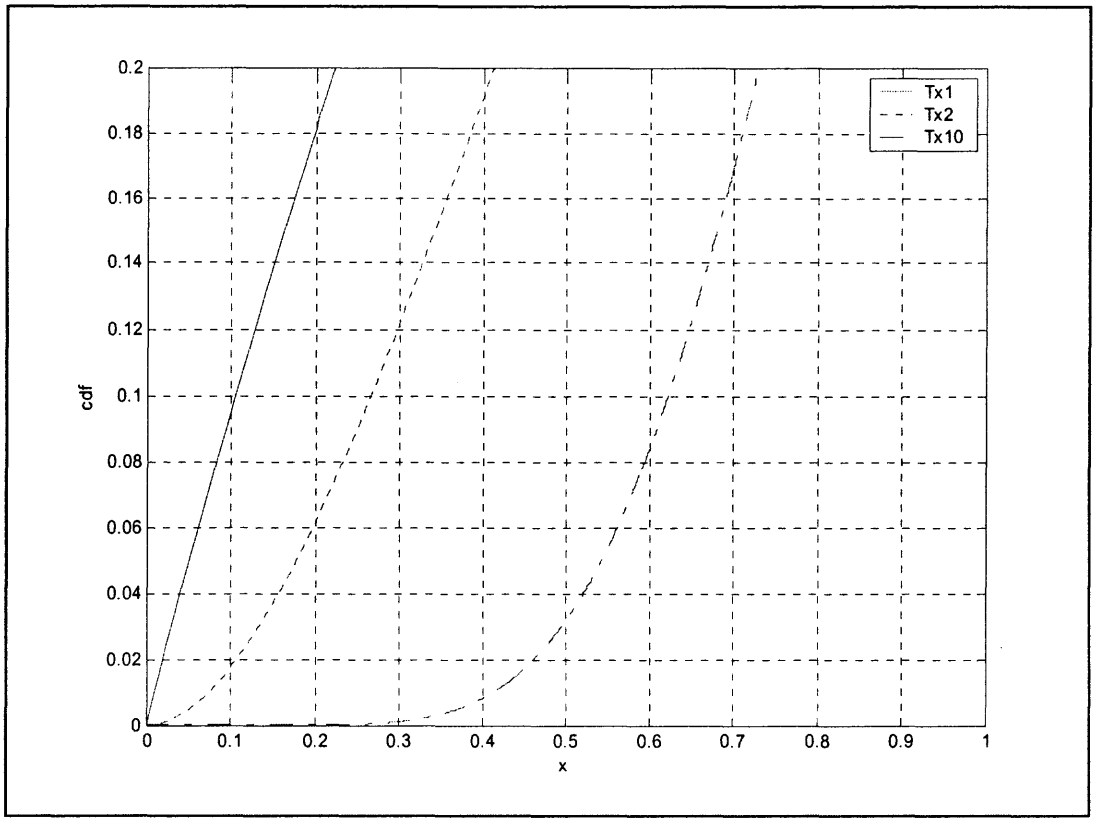

Figure 4.5 CDF plot of chi-square function

4.5 Impact of Code Length

The PSLR can be reduced by increasing the number of chips in a pulse. In Fig (4.5) gold codes of length 31 and 2047 were used. Two different environments were used first with a single transmitter and single receiver and in the second case with 10 transmitters and single receiver. Each of the transmitted signals sees different aspects of the stationary target. The comparisons were then made against 2 single pulse single transmitter cases. The two single pulse single transmitter cases, are again with target fluctuations and without.

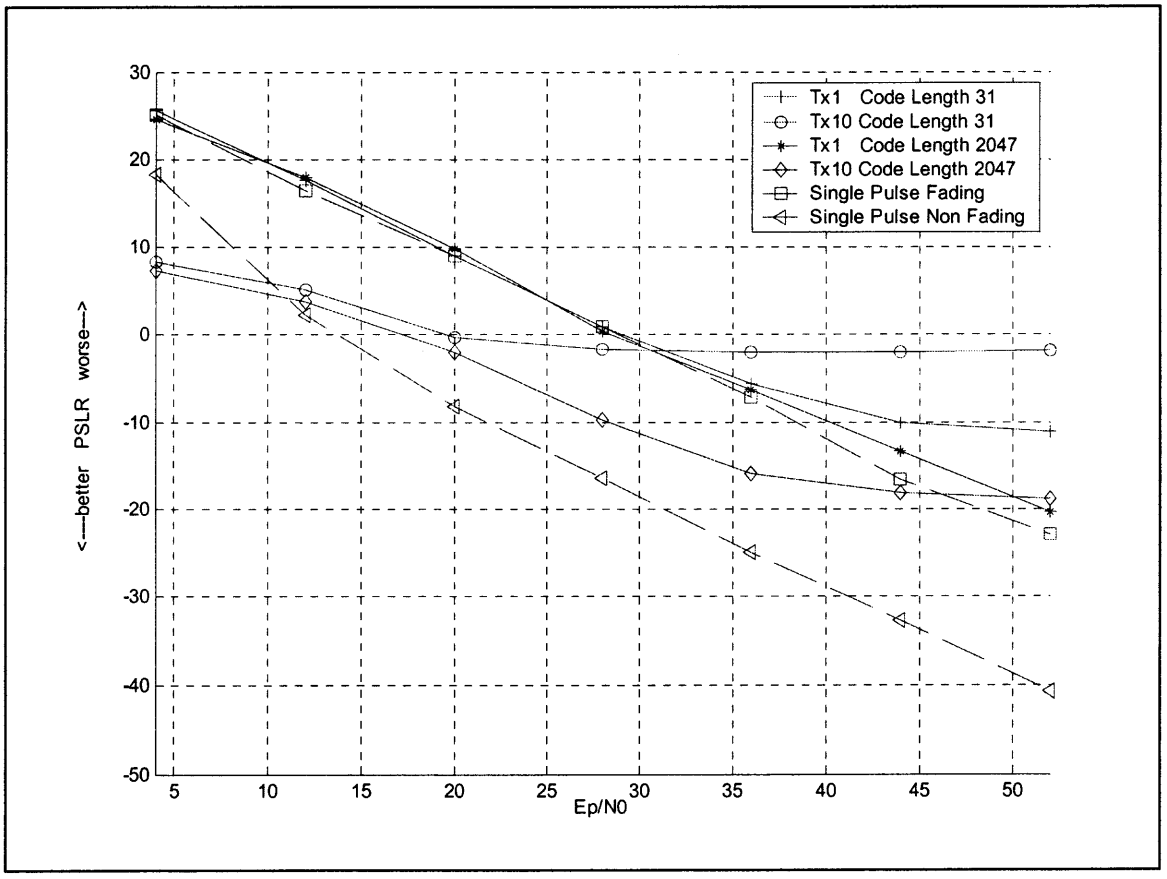

Figure 4.6 Multicode plot for PSLR of 99 percentile

Figure 4.5 represents the 99 percentile case which represents the worst case performance. The two single pulse scenarios act as a boundary. It can be inferred from Figure 4.3 that as the number of chips is increased i.e. code length from 31 to 2047, the PSLR approaches the Swerling 5 model i.e. the single pulse non-fading scenario. Increasing the code length reduces mutual interference, which allows the system to better capitalize on the diversity.

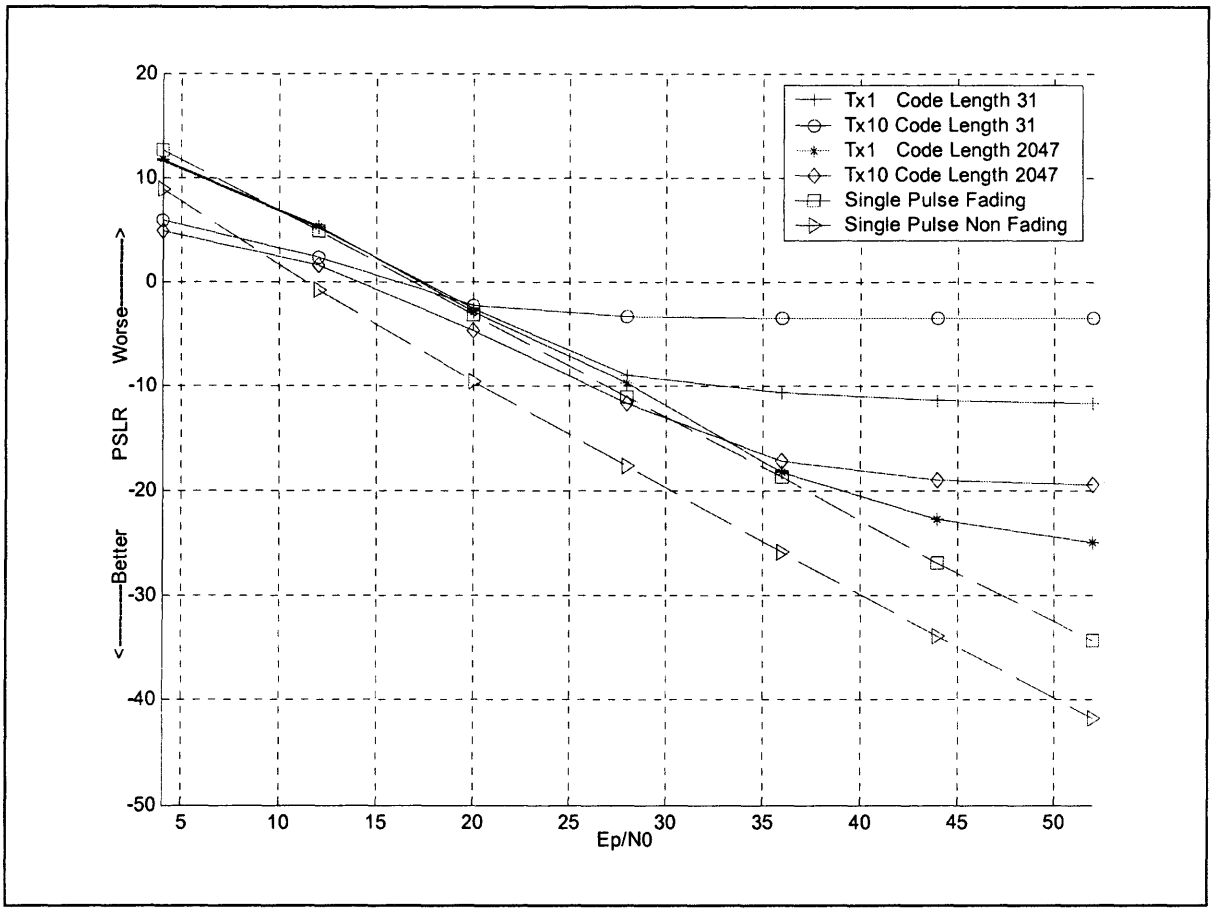

Figure 4.7 Multicode plot for PSLR of 85 percentile

Furthermore, the longer sequence leads to lower sidelobes in single transmitter case as the curves on the right hand side of Figure 4.6 can be observed.

4.6 Impact of Space Time Coding

In alamouti scheme each transmitter transmits two pulses. The two pulses are widely separated in time. At the receiver the pulses are processed such that the cross correlation is canceled. Orthogonality is maintained since the pulses are wide apart.

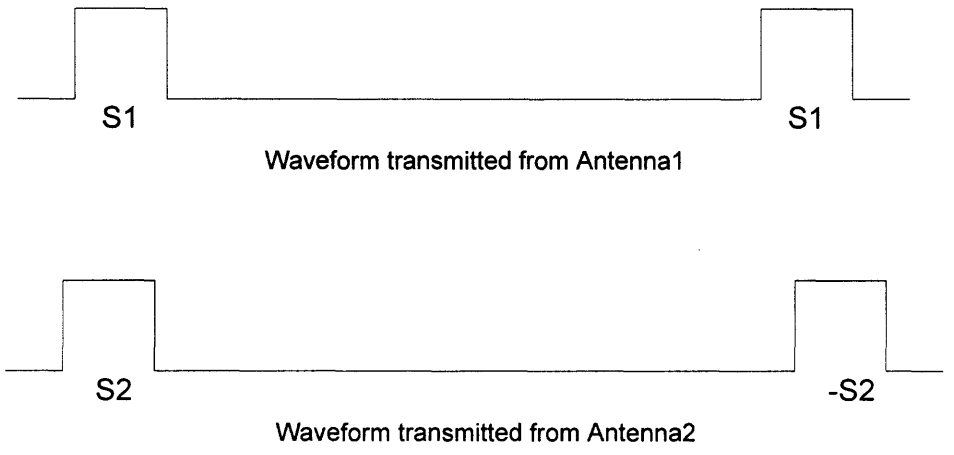

Figure 4.8 Space Time Codes

As shown in Figure 4.7 Transmitter-1 transmits pulses coded S1 and S1 with a wide time interval between them. Similarly Transmitter-2 transmits pulses coded S2 and -S2 with a wide time interval between them. In the space-time codes, the processing is done such that the cross correlation between the two codes are nullified, due to this they have a better performance. Figure (4.8) represents the 99 percentile plot of alamouti scheme for a gold code length of 127 and Figure (4.9) represents 99 percentile without alamouti scheme. It can be observed from the figures that in the alamouti scheme the cross correlation is cancelled, as the curves remain parallel even for high $\frac{E_p}{N_0}$ value .Thus operation range over which diversity is exploited is unlimited. In contrast, with the conventional scheme, diversity can be exploited over a limited range, as for high $\frac{E_p}{N_0}$ values the mutual interference limits the diversity gain.

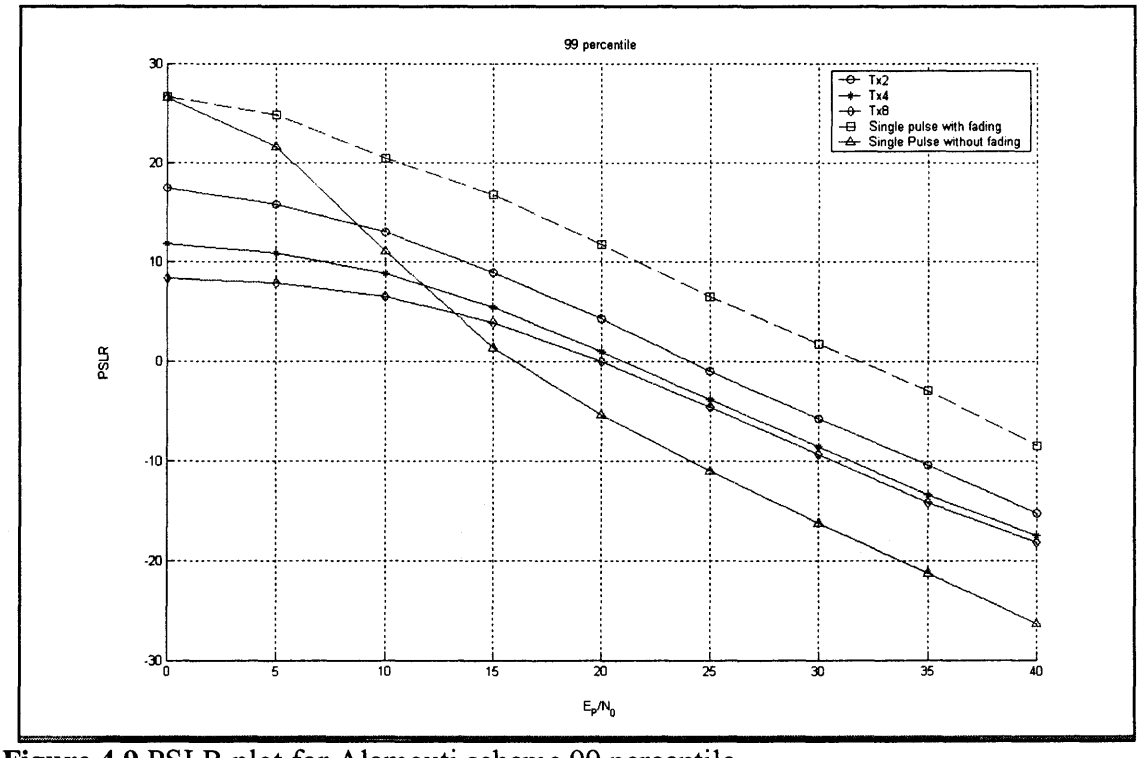

Figure 4.9 PSLR plot for Alamouti scheme 99 percentile

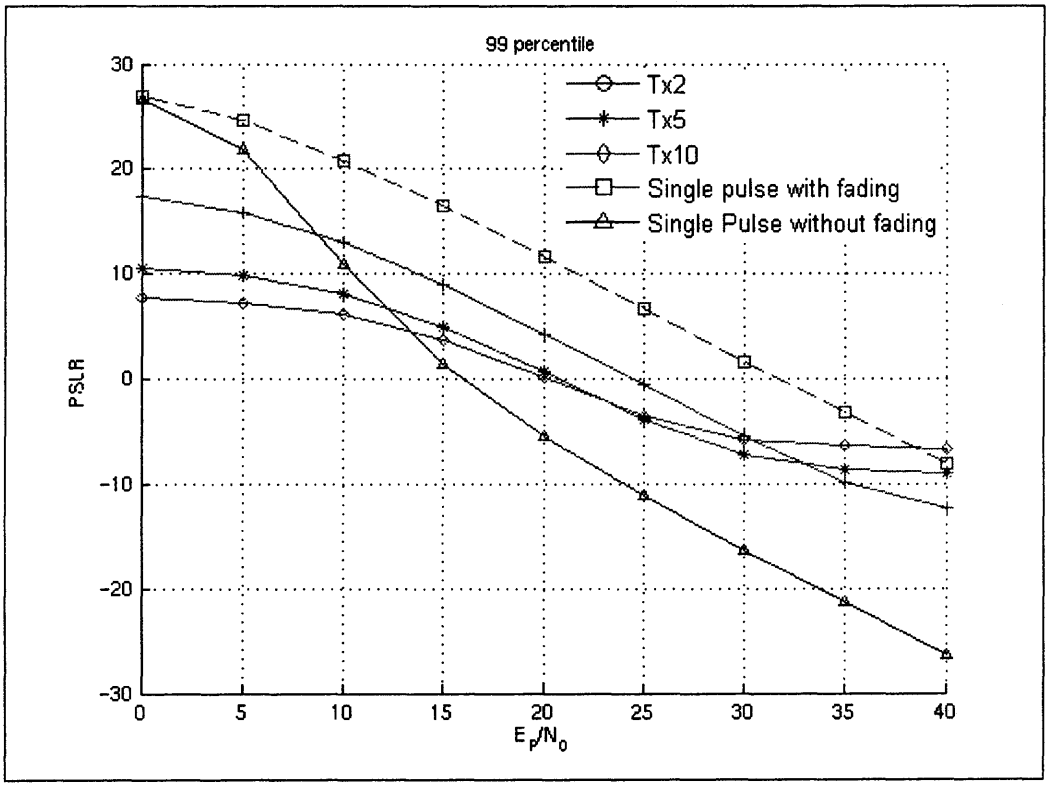

Figure 4.10 PSLR plot for 99 percentile of multiple transmitters.

4.7 Chi Square Distribution

The Purpose of this section is to explain how diversity affects the PSLR. Therefore, the statistics of the received signal energy, represented by the main lobe of the ambiguity function are analyzed given a certain number of transmitters. Each transmitted waveforms illuminates different aspects of the target. At the receiver, the output of each match filter is squared and summed. When independent normal variables are squared and added, it's a Chi square function with n degrees of freedom. Hence the main lobe of the ambiguity function follows a Chi square distribution.

Definition :

A Random variable X has a Chi square distribution (χ^2 distribution) with n degrees of freedom if its pdf is given by [19]

$$f(x)=\begin{cases}\dfrac{1}{\Gamma(\frac{n}{2})2^{n/2}}e^{-x/2}x^{n/2-1} & 0<x<\infty\end{cases} \tag{4.13}$$

The mean of a chi square distribution,

$$\mu = n \tag{4.14}$$

the variance of a chi square distribution,

$$\sigma^2 = 4n \tag{4.15}$$

In a MIMO Radar each channel is excited by a signal from transmitter, the code, with an amplitude $\frac{1}{\sqrt{2M}}$, where M is the number of transmit antennas. Each code sees a fading channel with a fading constant ζ . The ζ fading constant is a complex Gaussian with unit variance (σ^2 =1). Since the output of a matched filter is complex, hence the degrees of freedom of the output, the main lobe is given by equation (4.16)

$$2(\text{Number of transmitters}) = 2M \tag{4.16}$$

The mean of the main lobe of the ambiguity function is given by the equation (4.17) since it follows a Chi square distribution

$$\mu = 2M \tag{4.17}$$

and the variance of the main lobe

$$\sigma^2 = 4M \tag{4.18}$$

where N is the numbers of transmitters.

However the signal transmitted by m^{th} transmitter is scaled according to equation (4.19)

$$S_m = \frac{1}{\sqrt{2N}} S \tag{4.19}$$

The total Signal Energy received, E_p at the receiver is given by equation (4.18)

$$|S_r|^2 = \sum_i |S_m|^2 \tag{4.20}$$

$$|S_r|^2 = \sum_{m=1}^{M} \frac{1}{2M} |\zeta_m|^2 \tag{4.21}$$

$\sum |\zeta_i|^2$ follows a Chi square distribution the mean of the mean lobe

$$\mu = E\left\{|S_r|^2\right\} = \frac{2M}{2M} = 1 \tag{4.22}$$

The variance of the main lobe is given by

$$\sigma^2 = E\left\{(|S_r|^2 - \mu)^2\right\} = \frac{4M}{(2M)^2} = \frac{1}{M} \tag{4.23}$$

As can be seen from Equation (4.23), the variance is inversely proportional to the number of transmitters, and hence, if the number of transmitters is increased the power is

concentrated around the mean. Thus scaling in Equation 4.19 ensures that the total energy is constant independent of the number of transmitters.

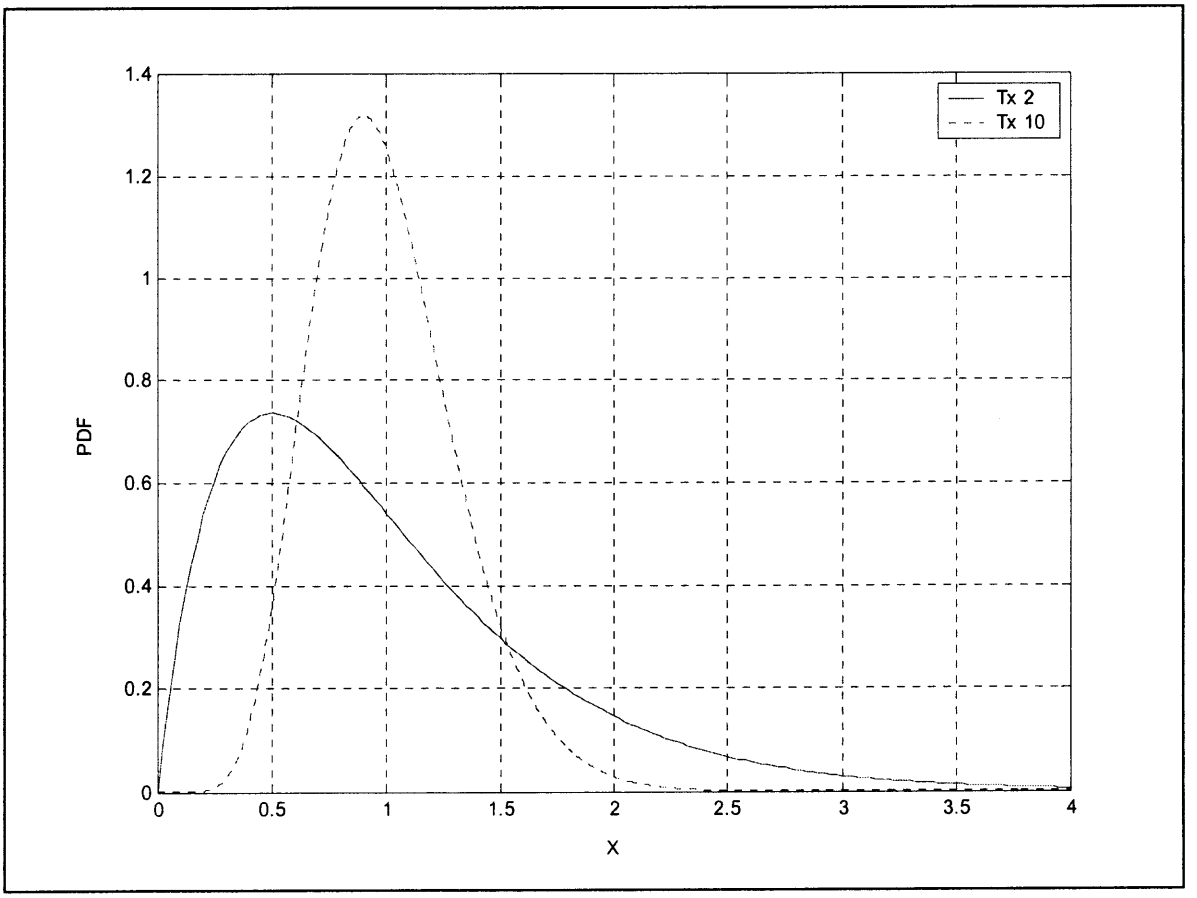

Figure 4.11 Chi square pdf function plot.

Figure 4.11 represents a Chi square function for 2 Transmitter and 10 Transmitter case. It can be observed that as the number of Transmitters is increased, the power is more concentrated. This is known as diversity gain. Hence, this proves that MIMO radar has diversity gain.

4.8 Impact of Multiple Transmitters on ISLR

ISLR (Integrated Sidelobe Ratio) is defined in chapter 2 and given by equation (2.19). ISLR is a measure of the area occupied by the sidelobes. It gives a measure of clutter and interferences. Figure (4.12) is a plot of ISLR for multiple transmitters for gold code length of 2047. It can be observed that as the number of transmitters is increased, ISLR is better at low $\frac{E_p}{N_0}$. Thus it can be concluded that the energy leaking from the main lobe into the sidelobes, is significantly reduced.

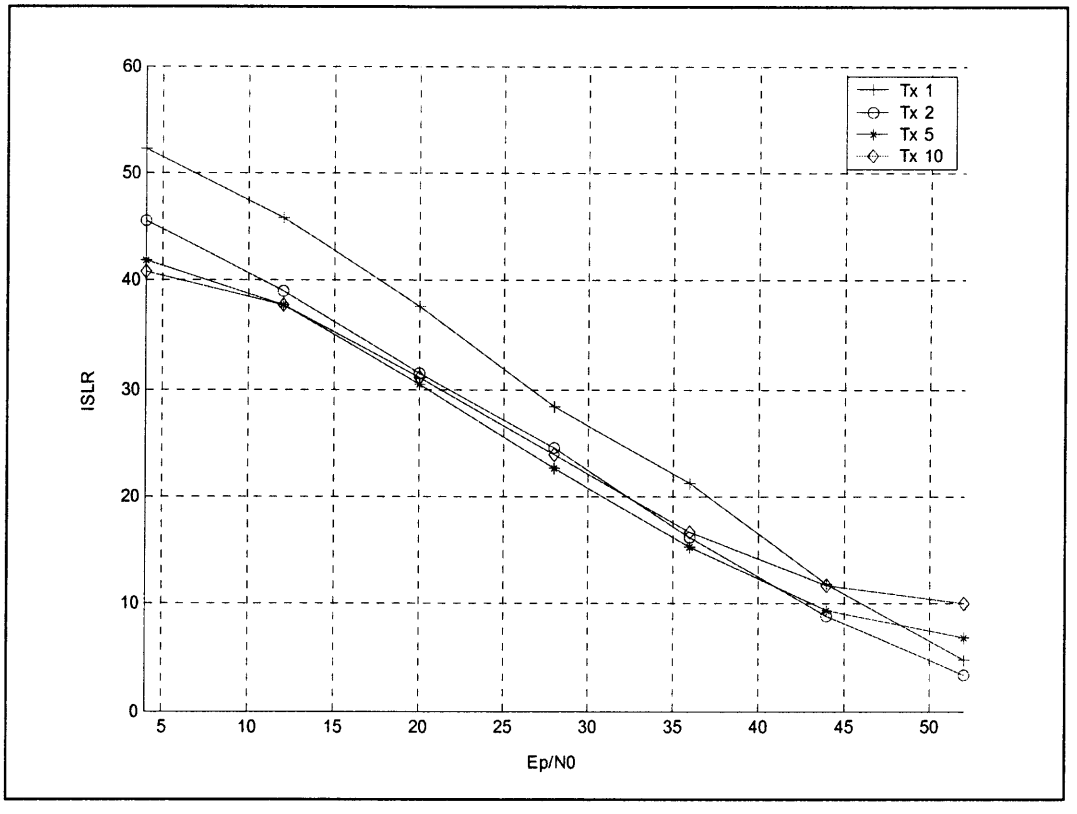

Figure 4.12 ISLR plot for Gold code length 2047 (99 percentile)

CHAPTER 5

CONCLUSION AND FUTURE WORK

MIMO Radar is a novel and ingenious method for target detection compared to conventional radar. Increase in the number of Transmitters leads to diversity gain. The results show that MIMO radar effectively utilizes diversity gain to reduce the PSLR considerably. Increase in the transmit signal code length further enhances the detection probability. However, using non-orthogonal codes like gold codes limit the SNR range over which the diversity gain can be utilized, due to mutual interference. Alamouti space-time coding scheme is introduced at the end of the thesis, which allows utilizing diversity without mutual interference and may, therefore, be particularly useful.

The work considered here is for zero Doppler case i.e. stationary targets and future work should include mobile targets. Also it has been assumed that all the reflected waves from the target arrive simultaneously at the receiver, although this may not be the case in real world scenario. Therefore, future work must devise a method to process the received waveforms arriving at different times.

REFERENCES

1. A. Mudukutore, V. Chandrasekar, R.J. Keeler, "Weather radars with pulse compression using complementary codes: simulation and evaluation," International Geoscience and Remote Sensing Symposium, May 1996. Volume 1, pp. 574-576.

2. B. R. Mahafza, A.Z. Elsherbeni, Simulations for Radar Systems Design, CRC Press, 2004.

3. A. K. Ojha, D.B. Koch, "Performance analysis of complementary coded radar signals in an AWGN environment," Proceedings of the IEEE Southeastcon '91, April 1991, Volume 2, pp. 842-846.

4. A .K. Ojha, D.B. Koch, "Impact of noise and target fluctuation on the performance of binary phase coded radar signals," Proceedings of the IEEE Southeastcon '92, April 1992, Volume 1, pp. 215-218.

5. A. M. D. Turkmani and U.S. Goni, "Performance evaluation of maximal-length, Gold and Kasami codes as spreading sequences in CDMA systems," Proceedings of 2nd International Conference on Universal Personal Communications, 1993, Oct 1993, Volume 2, pp. 970-974.

6. D. W. Bliss, K. W. Forsythe, "Multiple-input multiple-output (MIMO) radar and imaging: degrees of freedom and resolution," Thirty-Seventh Asilomar Conference on Signals, Systems and Computers, November 2003. Volume 1, pp. 54-59.

7. E. Fishler, A. Haimovich, R. Blum, D. Chizhik, L. Cimini, R. Valenzuela, "MIMO radar: an idea whose time has come" Proceedings of the IEEE Radar Conference, 2004, pp. 71-78.

8. E. Fishler, A. Haimovich, R. Blum, D. Chizhik, L. Cimini, R. Valenzuela, "Performance of MIMO radar systems: advantages of angular diversity," Proceedings of Thirty-Eighth Asilomar Conference on Signals, Systems and Computers, 2004. Volume 1, pp. 305-309.

9. J. A. Biddiscombe, S.P. Kingsley, "An investigation into the principles of signal detection using multiple simultaneous waveforms," IEE Colloquium on Advanced Transmission Waveforms, June 1995, pp. 1-7.

10. M. Dawood, R. M. Narayanan, "Ambiguity function of an ultrawideband random noise radar," IEEE International Symposium Antennas and Propagation Society, July 2000. Volume: 4, pp. 2142-2145.

11. M. J. E. Golay, "Complementary Series," IEEE Transactions on Information theory, April 1961. Volume: 2, pp. 82-87.

12. M. I. Skolnik, Introduction to Radar Systems, McGraw-Hill, 1980.

13. M. N. Cohen, M. R. Fox, J. M. Baden, "Minimum peak sidelobe pulse compression codes," IEEE International Radar Conference, May 1990. pp 633-638.

14. M. Jankiraman, Space-Time Codes and MIMO Systems, Artech House, 2004.

15. N. Levanon, Radar Principles, John Wiley and Sons, 1988.

16. N. Levanon, E. Mozeson, Radar Signals, John Wiley and Sons, 2004.

17. R. Sivaswamy, "Multiphase Complementary Codes," IEEE Transactions on Information Theory, Sep 1978. Volume 24, Issue: 5, pp 546-552.

18. T. B. Hale, M. A. Temple, B. L. Crossley, "Ambiguity analysis for pulse compression radar using Gold code sequences," Proceedings of the 2001 IEEE Radar Conference, May 2001, pp. 111-116.

19. V .K. Rohatgi, An Introduction to Probability Theory and Mathematical Statistics, 1976.

20. K. H. A.Karrakainen and P. A. Leppanen, "The Influence of Initial-Phases of a PN Code Set on the Performance of an Asynchronous DS-CDMA System," Wireless Personal Communications, Kluwer Academic Publication, 2000, pp. 279-293.

21. N. Lehmann, E. Fishler, A. Haimovich, R. Blum, D. Chizhik, L. Cimini, R. Valenzuela, "Evaluation of transmit diversity in MIMO-radar direction Finding," Submitted to IEEE Transactions on Aerospace and Electronic Systems.

22. P. M. Woodward, Probability and Information the theory with Applications to Radar, McGraw-Hill, 1953.